Thermodynamic Insights on the Feasibility of Homogeneous Batch Extractive Distillation. 3. Azeotropic Mixtures with Light Boiling Entrainer

Ivonne Rodríguez-Donis, Vincent Gerbaud, Xavier Joulia

Thermodynamic Insights on the Feasibility of Homogeneous Batch Extractive Distillation. 3. Azeotropic Mixtures with Light Entrainer.

Ivonne Rodriguez-Donis

Instituto Superior de Tecnologías y Ciencias Aplicadas (INSTEC), Avenida Salvador Allende Luaces, Plaza, Ciudad de la Habana, Cuba

Vincent Gerbaud* and Xavier Joulia

Université de Toulouse, INP, UPS, LGC (Laboratoire de Génie Chimique), 4 allée Emile Monso, F-31432 Toulouse Cedex 04, France
CNRS, LGC (Laboratoire de Génie Chimique), F-31432 Toulouse Cedex 04, France

ABSTRACT: This article shows how knowledge of the location of univolatility lines and residue curve analysis helps in assessing the feasibility of extractive distillation of minimum-boiling (minT) or maximum-boiling (maxT) azeotropic mixtures or low-relative-volatility (low-α) mixtures (A−B) by using a light-boiling entrainer (E), in accordance with the general feasibility criterion of Rodriguez-Donis et al. [*Ind. Eng. Chem. Res.* **2009**, *48* (7), 3544−3559]. Considering all possible locations of the univolatility line α_{AB}, three minT azeotropic mixtures with a light entrainer (1.0−2 class), namely, ethanol−water with methanol, ethanol−toluene with acetone, and methyl ethyl ketone−benzene with acetone; three maxT azeotropic mixtures with a light entrainer (1.0−1a class), namely, water−ethylenediamine with methanol, acetone−chloroform with dichlomethane, and propanoic acid−dimethyl formamide with methyl isobutyl ketone; and one low-α mixture with a light entrainer (0.0−1 class), namely, ethyl acetate−benzene with acetone, were studied in a stripping extractive column. For the 1.0−2 class, both A and B can be recovered as the bottom product, depending on the location of $\alpha_{AB} = 1$, which sets limiting values for the entrainer feed flow rate F_E/L_T for one of the product. In addition, the feasible region of the extractive distillation process is larger than for the azeotropic distillation process. For the 1.0−1a class, the product is either A or B, depending on the location of $\alpha_{AB} = 1$, which sets a minimum value of $(F_E/L_T)_{min}$ for one of the product. For the 0.0−1 class, feasibility depends on the existence $\alpha_{AB} = 1$. When it does not exist, B is the unique possible product. When it does, both A and B are products, with B below a maximum value of $(F_E/L_T)_{max,B}$ and A above a minimum value $(F_E/L_T)_{min,A}$.

1. INTRODUCTION

Distillation is part of 85% of industrial processes as a key process for product purification. For nonideal mixtures involving azeotropes or low relative volatilities, separation requires advanced distillation processes, such as azeotropic distillation, in which an entrainer is fed at the same tray (or vessel) as the mixture to be separated, and extractive distillation, in which the entrainer is fed at a different tray than the mixture to be split. Considering a nonideal binary mixture (A−B) where A is assumed to be more volatile than B, adding a third component [entrainer (E)] that selectively interacts with one of the original components can help draw the other component as a top or bottom product.

For extractive distillation, the industrial practice of finding a suitable entrainer (E) relies on the sole rule of selecting an entrainer that does not form any azeotropic mixture with the original components and is the heavy boiler for a minimum-boiling-temperature (minT) azeotrope separation or the light boiler for maximum-boiling-temperature (maxT) azeotrope separation. The restriction of not forming a new azeotrope is not a strict one,[1] but it has proved useful in industrial practice, particularly because it leads to the often-occurring ternary diagram (A−B−E) belonging to class 1.0−1a according Serafimov's classification (occurrence amounts to 21.6%).[2,3]

The performance of an extractive distillation process is strongly related to the entrainer selectivity.[4] Depending on whether it increases or decreases the A−B relative volatility, the distillate for the extractive distillation of minT azeotropes (A−B) with a heavy (light) entrainer is either the light- (heavy-) boiling component (A) or, counterintuitively, the intermediate-boiling component (B).[4,5] This behavior was explained by Laroche et al. by means of volatility order regions and the location of the univolatility curves.[4]

Over the years, the synthesis and design of extractive distillation, including which product is distilled first, the existence of a limiting entrainer flow rate, and limited recovery yields, has been methodically assessed by computing the liquid profile in each column section by a discrete[6] or continuous[7,8] model. A more general trend based on thermodynamic insight alone was suggested by Laroche et al.[4] and Knapp and Doherty[9] to design extractive distillation process. Recently, a general feasibility criterion suitable under an infinite-reflux/-reboil operation and an infinite number of stages and combining the existence and location of the univolatility line along with the contour of the residue curves was reported by Rodriguez-Donis et al.[10] in part 1 of this article series. Parts 1[10] and 2[11] discussed the application of the general feasibility criterion to the separation of minT or maxT

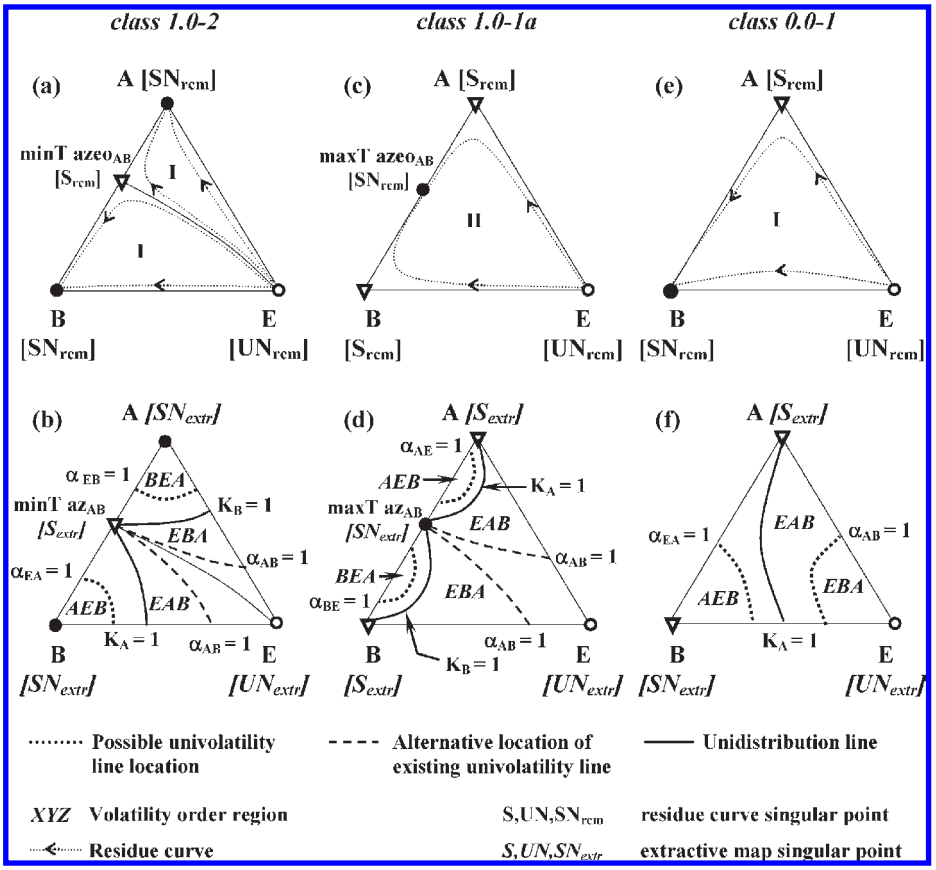

Figure 1. Residue curve map and unidistribution and univolatility lines for all ternary diagrams involved in the homogeneous extractive distillation process using light entrainers.

azeotropic mixtures and low-relative-volatility mixtures, respectively, using a heavy entrainer in either batch rectifying or stripping column configurations.

The application of light- and intermediate-boiling entrainers in extractive distillation has been well-studied. Extractive distillation using an intermediate entrainer is suitable for the separation of an azeotropic mixture in which the boiling temperatures of the compounds are not too close.[5] A light entrainer can offer an attractive alternative to a heavy entrainer for separating azeotropic or low-relative-volatility mixtures because the process might require less energy. Indeed, for continuous extractive distillation, based on the study of 416 binary mixtures with a light entrainer, Laroche et al.[5] demonstrated that light entrainers are as common as heavy entrainers and, in some cases, can perform as well as or better than heavy entrainers. For instance, the separation of ethyl acetate−methyl ethyl ketone using the light entrainer acetone requires lower solvent-to-feed and reflux ratios than that using the heavy entrainer toluene.

In this article, we methodically study the use of low-boiling entrainers without inducing a new azeotrope for separating azeotropic and close-boiling mixtures by extractive distillation, in light of the new general feasibility criterion reported in part 1.[10]

Separation of a minT azeotrope with a light entrainer leads to Serafimov's class 1.0−2 ternary diagram (8.5% occurrence among azeotropic diagrams[3]), separation of a maxT azeotrope with a light entrainer leads to Serafimov's class 1.0−1a ternary diagram (21.6% occurrence[3]), and separation of a low-relative-volatility binary mixture with a light entrainer corresponds to Serafimov's class 0.0−1 (Figure 1). We illustrate our study by considering batch distillation, but the feasibility analysis based on thermodynamic insight holds for continuous operation as well. Ternary mixtures reported in the literature were taken as test mixtures. The general feasibility criterion under an infinite reflux was checked systematically and confirmed by computing composition

Table 1. Binary Coefficients (cal/mol) for Computing Ternary Liquid−Vapor Equilibria Obtained Using the NRTL Model

	A_{ij}	A_{ji}	α_{ij}
methanol (E)−ethanol (A)	−25.9969	12.7341	0.3356
methanol (E)−water (B)	−253.88	845.206	0.2994
ethanol (A)−water (B)	−635.56	1616.81	0.1448
acetone (A)−MEK (B)	−66.7019	22.1895	0.3031
acetone (A)−benzene (E)	−193.34	569.931	0.3007
MEK (B)−benzene (E)	−308.999	508.223	0.2847
methanol (E)−water (A)	−253.88	845.206	0.2994
methanol (E)−EDA (B)	524.626	−1290.36	0.3087
water (A)−EDA (B)	405.224	−1012.63	0.7907
acetone (E)−ethyl acetate (A)	−153.477	235.069	0.2910
acetone (E)−benzene (B)	−193.340	569.931	0.3007
ethyl acetate (A)−benzene (B)	−273.017	383.126	0.3196

profiles under both infinite and finite reflux conditions, considering the light entrainer fed as a saturated vapor or a liquid. Further validation was done by rigorous simulation.

Univolatility and unidistribution lines, residue curve maps, singular-point stability, and rectifying and extractive composition profiles at a given reflux ratio and entrainer flow rate were computed with RegSolResidue and drawn with the freeware ProSim Ternary Diagram.[12] Stripping profiles were computed with Simulis Thermodynamics[13] in Microsoft Excel. The nonrandom two-liquid (NRTL) thermodynamic model was used for computing the liquid−vapor equilibrium. Binary coefficients were taken from the literature[14] or determined from estimated binary data using the universal functional activity coefficient method (UNIFAC) and are listed in Table 1. Rigorous simulations were performed with both ProSim BatchColumn[15] and CHEMCAD,[16] using the following assumptions: theoretical plates, negligible liquid holdup on the trays, no pressure drop inside the column, adiabatic column operation, vapor- or liquid-saturated entrainer fed at an intermediate tray, and top-vessel liquid kept at boiling temperature.

2. STATE OF THE ART

Hunek et al. were the first to simulate the separation of a multicomponent mixture involving water and C1−C4 alcohols with use of a light entrainer, methanol, in a sequence of continuous distillation columns.[17] Calling the process reverse extractive distillation, they were able to distill the lightest alcohols from water thanks to a large amount of methanol in the main feed. In an article published in 1992, Laroche et al. noticed unusual behaviors of azeotropic and extractive distillation of minT azeotropes compared to zeotropic distillation.[5] In particular, the extractive distillation of ethanol (A)−water (B) with the light entrainer acetone (E) led to recovery of the intermediate-boiling ethanol (A) in the column bottom stream, instead of the heavy-boiling water (B), as would have been expected.[5] An explanation based on the univolatility curve and volatility order region given in 1991 by the same authors in an article titled "Homogeneous Azeotropic Distillation: Comparing Entrainers". The article title is misleading as it provides explanation that concerns extractive distillation as well.[4] For minT azeotrope separation with a light entrainer (E) fed together with the main feed (diagram 1.0−2), they concluded that pure B (A) can be recovered in the bottom stream of the extractive continuous distillation column in case 1 (case 2) when B (A) is the least volatile component in the region where apex E lies as well. Illustrative mixtures were ethanol (A)−water (B) with the light entrainer acetone (E) for case 1 and methyl ethyl ketone (A)−water (B) with the light entrainer acetone (E) for case 2. The general criterion of Rodriguez-Donis et al.[10] fully corroborates this analysis by simultaneously combining the relationship between the residue curve map and the location of the univolatility line. Until the present article, extension for all ternary diagrams including minT and maxT azeotropes and low-relative-volatility (close-boiling) mixture has not been not investigated systematically for light entrainers.

In batch operation, the separation of the minT azeotrope ethanol (A)−water (B) using the light entrainer methanol (E) (1.0−2 diagram) has kept the attention of most authors. Lelkes et al.[18] studied an extractive batch rectifier and obtained a water-free mixture of methanol and ethanol as the distillate product when feeding the light entrainer continuously into the still during the whole operation and keeping a low reflux ratio so as to allow extractive profiles to cross the distillation boundary typical of the 1.0−2 diagram (see Figure 1). The main drawback was the high

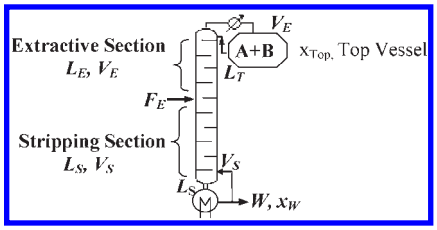

Figure 2. Batch stripping column for homogeneous extractive distillation processes using light entrainers.

consumption of entrainer and the pollution of the distillate by the entrainer, which required further purification steps. Based on these results, similar analyses were done for the separation in a batch rectifier of a maxT azeotrope [water (A)−ethylene diamine (B) with methanol (E)] and a close-boiling binary mixture [chlorobenzene (A)−ethylebenzene (B) with 4-methylheptane (E)].[6,18,19] Regarding the position for feeding the entrainer, the best results for a batch rectifier were always obtained with continuous introduction into the boiler, with separation taking place with a single rectifying column section. A parametric study to determine the applicable ranges for the reflux ratio, entrainer feed ratio, and stage number in each column section was also performed.[19]

Lang et al.[20] were the first to propose using a batch stripper as shown in Figure 2, feeding E as a saturated vapor and allowing the withdrawal of pure water (B) from the bottom instead of an E−A mixture from the rectifier. Being a stable node of the residue curve map, water can be recovered without any entrainer feeding in a stripper column, but the use of extractive distillation increases the size of the feasible region. For batch extractive distillation, Lang et al. extended the simplified model proposed by Lelkes et al.[21] for computing the maps of liquid profiles inside the extractive and stripping sections of the batch stripping column (Figure 2). They used these maps to determine the minimum and maximum feasible ratios of the entrainer flow rate to the top liquid feed rate (F_E/L_T) and the minimum-boiler reflux ratio S. Theoretically, the feeding of light entrainer as a saturated vapor in a batch stripper can be considered as the opposite case of feeding a heavy entrainer as a boiling liquid in a batch rectifying column configuration, but equations for the saturated vapor feed were not published. Under a finite reboil ratio, bottom product withdrawal was possible above a minimum reboil ratio S, as explained for another mixture, butanol (A)−butylacetate (B) with the light entrainer dipropylether (E).[20] Varga[22] derived all of the equations relevant to a batch stripper and studied the separation of the maxT azeotrope water (A)−ethylenediamine (B) using methanol (E) as a light entrainer in a batch stripping column in which the initial binary mixture was fully charged into the top vessel. The entrainer was considered as a boiling liquid, and influence of the position of the entrainer feed on the process feasibility was studied systematically: (a) at the column top, (b) at an intermediate plate, and (c) at the bottom of the column. In case a, only a stripping section exists; in case b, there are two sections, namely, extractive and stripping; and in case c, there is a unique extractive section. The best results were obtained for case b, but rigorous simulation at $S \approx 55$ and $F_E/L_T = 2$ showed that, after 10 h, the main component of the bottom product was ethylenediamine but it was still polluted with 5% of methanol, at the expense of very high entrainer consumption. At least the stripper extractive configuration led to a simpler and more efficient separation than the rectifier configuration studied

earlier for the same mixture by the same author and colleagues.[19] At $S_{min} = 8.1$ for $F_E/L_T = 1$, with an initial azeotropic mixture, the process became unfeasible because the unstable extractive separatrix created a large unfeasible region inside the triangle, as observed earlier.[20]

None of these previous studies in batch extractive distillation with a light entrainer considered the effect of the univolatility lines on the feasibility of the process or the ease with which it could be completed.

3. EQUATIONS FOR COMPUTING THE EXTRACTIVE LIQUID PROFILE IN A BATCH STRIPPER

Figure 2 displays a batch stripper column configuration. The original binary mixture (A−B) is initially charged into the column top vessel and goes to the first top tray as a boiling liquid (L_T). Light entrainer (F_E) is introduced continuously at an intermediate tray, leading to two column sections: extractive and stripping. Partial evaporation of the liquid phase reaching the column bottom gives the vapor flow rate (V_S). The remaining liquid is drawn as bottom product (W) to maintain the liquid amount in the boiler.

Variations of the top-vessel liquid holdup U_{Top} and composition x_{Top} are computed by a material balance

$$\frac{dU_{Top}}{dt} = F_E - W \tag{1}$$

$$\frac{dx_{Top}}{dt} = \frac{F_E}{U}(x_E - x_{Top}) + \frac{W}{U}(x_{Top} - x_W) \tag{2}$$

The liquid composition profile in each column section is computed by using the general differential model of Lelkes et al. with constant molar overflow assumptions,[18] once a composition of the bottom product x_W has been chosen

$$\frac{dx_i}{dh} = \frac{V}{L}(y_i - y_i^*) \tag{3}$$

In eq 3, y_i^* and y_i are the equilibrium composition with x_i and the operating composition computed from material balance for a given tray, respectively. Depending on the section, the V/L ratio in eq 3 is labeled with subscript E (extractive) or S (stripping). Considering the feed physical state by the variable q [boiling liquid ($q = 1$) or saturated vapor ($q = 0$)] and defining the reboil ratio S, one obtains

$$V_S = SW \tag{4}$$

$$V_E = V_S + (1 - q)F_E \tag{5}$$

$$L_E = L_T \tag{6}$$

$$L_S = V_S + W = L_E + qF_E \tag{7}$$

Then, for a boiling liquid F_E ($q = 1$), y and V/L become

$$y|_{q=1} = \frac{x + \left(\frac{F_E}{L_T}\right)x_E - \left(\frac{1}{S+1}\right)\left(1 + \frac{F_E}{L_T}\right)x_W}{\left(\frac{S}{S+1}\right)\left(1 + \frac{F_E}{L_T}\right)} \tag{8}$$

$$\left.\frac{V}{L}\right|_{q=1} = \left(\frac{S}{S+1}\right)\left(1 + \frac{F_E}{L_T}\right) \tag{9}$$

and for a saturated vapor F_E ($q = 0$)

$$y|_{q=0} = \frac{x + \left(\frac{F_E}{L_T}\right)x_E - \left(\frac{1}{S+1}\right)x_W}{\left(\frac{S}{S+1} + \frac{F_E}{L_T}\right)} \tag{10}$$

$$\left.\frac{V}{L}\right|_{q=0} = \left(\frac{S}{S+1} + \frac{F_E}{L_T}\right) \tag{11}$$

Under an infinite reboil ratio, pairs of eqs 8 and 10 and 9 and 11 become identical regardless of the feed state. Therefore, the extractive liquid composition maps are similar, and the process limiting entrainer flow rate is identical considering the entrainer as a saturated liquid or vapor.

The stripping composition profiles are computed by setting $F_E = 0$. Under an infinite reboil ratio S_∞, they become equivalent to the residue curve equation

$$\frac{dx_i}{dh} = (x_i - y_i^*) \tag{12}$$

The liquid profile of the extractive section starts at the composition of the top vessel (x_{Top}) and ends at an unstable extractive node. The stripping profile then makes a connection between the stable extractive node, SN_{extr}, and the liquid composition in the boiler, x_W. The extractive batch distillation process is considered to be feasible when a set of operating conditions allows a continuous liquid profile in the column from x_{Top} to x_W that combines an extractive section composition profile $\{x_{Top} - SN_{extr}\}$, SN_{extr} located at the entrainer feeding plate, and a stripping section composition profile $\{SN_{extr} - x_W\}$ assimilated to a residue curve at S_∞.

4. FEASIBILITY CRITERION FOR THE SYNTHESIS OF HOMOGENEOUS EXTRACTIVE DISTILLATION PROCESSES IN A BATCH STRIPPER

Being a light boiler, the entrainer is always the residue curve unstable node, UN_{rcm} (white circle), whereas A or/and B are residue curve stable node(s) SN_{rcm} (black circle) or saddle point(s), S_{rcm} (white downward-pointing triangle) according to the three residue curve maps displayed in Figure 1. That makes the use of a rectifying column configuration for the withdrawal of pure component A or B in the distillate impossible. Instead, a stripper configuration as in Figure 2 must be considered.

Figure 1 summarizes the topological features (singular points, unidistribution lines $K_i = 1$, univolatility lines $\alpha_{ij} = 1$, and volatility order regions) of ternary diagrams 1.0−1a, 1.0−2, and 0.0−1 corresponding to the separations of a maxT azeotrope, a minT azeotrope, and a low-relative-volatility mixture, respectively, with a light entrainer. Panels b and d of Figure 1 make the necessary distinction for the $\alpha_{AB} = 1$ alternative locations for the 1.0−2 and 1.0−1a classes, respectively. For extractive distillation in a rectifier configuration when using a heavy entrainer,[10,11] the stabilities of the singular points of the residue curve map (rcm) and of the extractive liquid profile map (extr) are opposite because the ending point of the extractive composition profile, SN_{extr}, lies at the residue curve unstable node, UN_{rcm}, at the limit $F_E \rightarrow 0^+$.[9] Here, with a stripping configuration, the stabilities of the residue curve map and of the extractive profile map at the limit $F_E \rightarrow 0^+$ are the same: $UN_{rcm} = UN_{extr}$, etc.

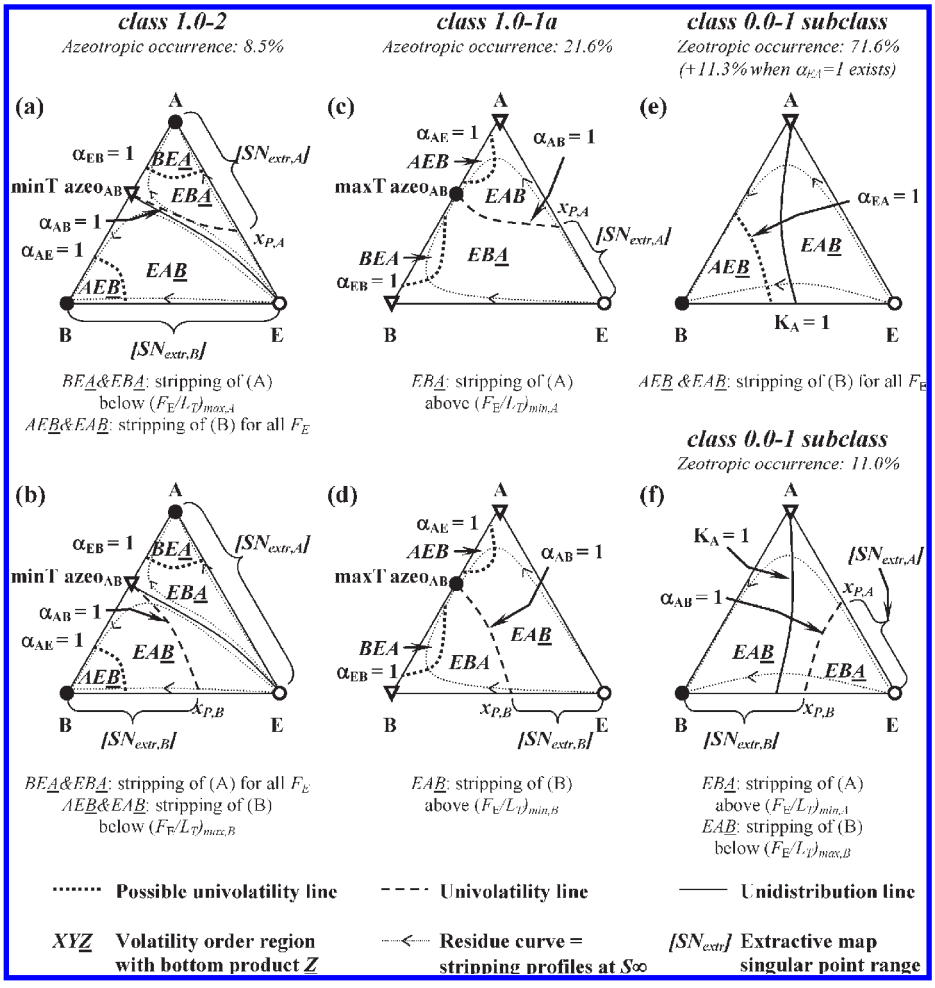

Figure 3. Thermodynamic features relative to the feasibility of extractive distillation in a stripper using light entrainers for ternary diagrams 1.0−1a, 1.0−2, and 0.0−1.

4.1. Feasibility under an Infinite Reboil Ratio. From the topological features displayed in Figure 1, application of the general feasibility criterion described in part 1[10] enables the feasibility of homogeneous extractive distillation for a stripper configuration under an infinite reboil ratio to be checked. As stated in ref 10, "Component A or B can be drawn as [the] first bottom product using a stripper configuration if there is a residue curve going from the entrainer E towards A or B and following an increasing temperature in the region in which A or B is the least volatile component of the ternary mixture". We note that this criterion holds not for azeotropic distillation but only for extractive distillation. Consider class 1.0−1a (Figure 1c,d). Regardless of the location of the univolatility line, azeotropic distillation in a stripper will recover the maxT azeotrope in the bottom because it is the unique stable node of the residue curve map, SN_{rcm}. In contrast, applying the general criterion for extractive distillation in a stripper, that is, locating the volatility order regions related to the univolatility line, enables one to determine whether A or B is the bottom product (Figure 3), which is impossible in azeotropic distillation because both A and B are saddle points.

The possible bottom products in each volatility order region depend on the location of the univolatility line $\alpha_{AB} = 1$ and its intersection x_P with the triangle edge and are summarized in Figure 3.

The 1.0−2 class of ternary diagrams (Figure 1a,b) concerns the separation of minT azeotropes with light entrainers. The stabilities of both A and B are SN_{rcm} and SN_{extr}, and the light entrainer E is UN_{rcm} and UN_{extr}. The residue curve map is split into two distillation regions by a distillation boundary. There are also two unidistribution lines (K_A, K_B) corresponding to each azeotropic component, and all three univolatility lines can occur. There are two locations of $\alpha_{AB} = 1$ inverting the volatility order between A and B, and therefore, two cases are considered when dealing with extractive distillation (Figure 3a,b).

According to Figure 3a,b, both components A and B can be recovered as bottom products, because they satisfy the general feasibility criterion: In volatility order regions BE<u>A</u> and EB<u>A</u>, A is the least volatile component, is connected to E by a residue curve in the direction of increasing temperature, and is a product (denoted in Figure 3 as <u>A</u>). In volatility order regions AE<u>B</u> and EA<u>B</u>, the same occurs for B, which is the bottom product. Univolatility curves α_{EA} and α_{EB} do not affect the A versus B volatility order and, therefore, do not affect the expected product.

Class 1.0−1a ternary diagrams (Figure 1c,d) concern the separation of maxT azeotropes with light entrainers. The stabilities of both A and B are S_{rcm} and S_{extr}, and light entrainer E is UN_{rcm} and UN_{extr}. Two unidistribution lines, K_A and K_B, and three univolatility curves exist. Again, there are two locations of $\alpha_{AB} = 1$, and therefore, two cases are considered when dealing

with extractive distillation (Figure 3c,d). Application of the feasibility criterion shows that, when $\alpha_{AB} = 1$ intersects the A−E edge, Figure 3c (B−E edge, Figure 3d), A (B) is the bottom product in the volatility order region EBA (EAB).

For a 0.0−1 mixture (low-relative-volatility mixture with a light entrainer), the unidistribution line K_A always exists, but subclasses must be distinguished regarding the possible occurrence of univolatility lines $\alpha_{AB} = 1$ or $\alpha_{EA} = 1$: Reshetov's statistics mostly distinguish diagrams with no univolatility line (71.6% zeotropic occurrence, Figure 3e), with univolatility line $\alpha_{AB} = 1$ only (11.0% zeotropic occurrence, Figure 3f), and with univolatility line $\alpha_{EA} = 1$ only (11.3% zeotropic occurrence).[23] The case of a 0.0−1 mixture with $\alpha_{EA} = 1$ only behaves similarly to the 0.0−1 case with no univolatility line and is not further described. When no univolatility line $\alpha_{AB} = 1$ exists (Figure 3e), B is the bottom product in the volatility order region EAB. When the univolatility line $\alpha_{AB} = 1$ exists (Figure 3f), both A and B can be recovered as bottom products, A in the volatility order region EBA and B in the volatility order region EAB.

Finally, for all mixtures, the locations of the unidistribution lines are strongly connected to the residue curve shapes, as any $K_i = 1$ line intersects residue curves at composition extrema x_i.[2,3] Therefore, the locations of these lines also hint at the ease of the separation, particularly in terms of the reboil ratio and the number of theoretical stages required in each column section.

4.2. Influence of the Entrainer Flow Rate Ratio on Feasibility. The extractive profile map depends on the entrainer flow rate and the reflux parameters, and they affect the feasibility. A detailed analysis was given for the 1.0−1a class in the literature.[10,24] Under an infinite reboil ratio and a small entrainer flow rate ($F_E/L_T \rightarrow 0^+$) (Figure 1), the singular points of the extractive profile map are the same as the singular points of the residue curve map and have the same stability. As the entrainer flow rate increases, the extractive singular points move toward the entrainer vertex. Those at apexes (e.g., SN_{ext} in Figure 1a or S_{extr} A and B in Figure 1c) move along the triangle edge. Those located on the univolatility curve $\alpha_{AB} = 1$ move along it (e.g., S_{extr} minT $azeo_{AB}$ in Figure 1a and SN_{extr} maxT $azeo_{AB}$ in Figure 1c). Ultimately, SN_{extr} and S_{extr} can merge at the sacrifice of the extractive singular point being on the triangle edge.[9,10,24]

Recall that SN_{extr} must be present near the triangle edge to enable the intersection of the stripping and extractive section profiles and, thus, the feasibility of the process.

Applied to the 1.0−1a class, Figure 3c (Figure 3d), the merging of S_{extr} coming from apex A (B) with SN_{extr} coming from the maxT $azeo_{AB}$ leaves a persistent SN_{extr} above a minimum entrainer flow rate of $(F_E/L_T)_{min,A}$ $[(F_E/L_T)_{min,B}]$. That is, there is a limiting parameter for the process to be feasible and recover the feasible product A (B) when $\alpha_{AB} = 1$ intersects the A−E (B−E) edge, Figure 3c (Figure 3d). This result is parallel to the well-known minimum entrainer limit ratio occurring for the separation of a minT azeotrope with a heavy entrainer that also belongs to the 1.0−1a class.[7,9,10]

For the 1.0−2 class, there is no limiting entrainer flow rate to recover B (A) but there is a maximum entrainer flow rate $(F_E/L_T)_{max,A}$ $[(F_E/L_T)_{max,B}]$ to recover A (B) when $\alpha_{AB} = 1$ intersects the A−E (B−E) edge, Figure 3a (Figure 3b). Indeed, above this value, $SN_{extr,A}$ ($SN_{extr,B}$) disappears, merged with S_{extr} from the minT $azeo_{AB}$ in Figure 3a (Figure 3b). Similar behavior was described for the separation of a maxT azeotrope with a heavy entrainer that belongs also to class 1.0−2.[10]

The behavior 0.0−1 diagrams combines those of both 1.0−1a and 1.0−2 diagrams. There is a minimum entrainer flow rate to recover A and a maximum to recover B when $\alpha_{AB} = 1$ occurs (Figure 3f) and no limit when it does not occur (Figure 3e). Similar behavior was described for the separation of low-relative-volatility mixture with a heavy entrainer that also belongs to class 0.0−1.[11]

Further refining the analysis for class 1.0−2, three peculiarities occur. First, notice in Figure 3a (Figure 3b) the possible location range of the extractive stable node $SN_{extr,A}$ ($SN_{extr,B}$). Even if, theoretically, there is no limiting entrainer flow rate for recovery of B (A) because the extractive unstable node $SN_{extr,B}$ ($SN_{extr,A}$) can be located at any position on the B−E (A−E) edge, in practice, the existence of $(F_E/L_T)_{max,A}$ for A $[(F_E/L_T)_{max,B}$ for B] sets the existence of a minimum entrainer flow rate $(F_E/L_T)_{min,B}$ $[(F_E/L_T)_{min,A}]$ for B (A). Second, recovery of either A exclusively or B exclusively, or both components depends on the position of the univolatility line α_{AB} and the operating conditions. The same event was observed in the separation of maxT with a heavy entrainer, as discussed in detail in part 1 of this series.[10] Third, two stripping profiles under an infinite reboil ratio allow a feasible process for recovery of B (A) in each corresponding region. One stripping profile matches a residue curve going directly from E to apex B (A) close to the B−E (A−E) edge. The other matches a residue curve arriving at apex B (A) after nearing the saddle binary azeotrope minT $azeo_{AB}$. Which stripping profile will occur in reality depends on the operating parameters of the process such as the number of equilibrium stages, entrainer feeding tray, entrainer flow rate, and reboil ratio. This will be illustrated in the next section.

4.3. Influence of the Finite Reboil Ratio on Feasibility. At finite reflux/reboil, because of distillate or bottom product removal, extractive singular points, and residue curve map points as well, might move inside the triangle. They define unstable extractive and residue curve separatrices that set the feasible and unfeasible regions. Their occurrence can be predicted from simple knowledge of the ternary diagram class, but their precise locations are found by computing composition profiles, as in this article, or by numerical methods, such as homotopy continuation[9] or interval methods.[24] This is discussed in the examples of the next section.

5. SEPARATION OF MINIMUM-BOILING-TEMPERATURE AZEOTROPES WITH LIGHT ENTRAINERS (1.0−2 CLASS)

In the 1.0−2 diagram (Figure 1), both A and B are stable nodes SN_{rcm}, but they lie in two different distillation region. Therefore, unless the distillation boundary is highly curved, they cannot be recovered sequentially in a batch stripper by an azeotropic distillation process.[25,26] Extractive distillation is a worthwhile alternative process because extractive profiles can cross the distillation boundary of the residue curve map.

5.1. Ethanol (A)−Water (B) minT Azeotrope with Methanol (E). $\alpha_{AB} = 1$ Intercepts the A−E Edge. Separation of the ethanol (78.3 °C)−water (100.0 °C) minimum-boiling azeotrope (78.1 °C at $x_{ethanol} = 0.90$) with methanol (64.7 °C) fed as a boiling liquid ($q = 1$) is the most studied case.[5,6,17,19] The ternary diagram belongs to the 1.0−2 class (Figure 4a) and shows that the univolatility line $\alpha_{AB} = 1$ line intercepts $x_{P,A}$ at the methanol−ethanol edge (A−E) close to the ethanol apex. The general feasibility criterion states that water (B) can be recovered by a

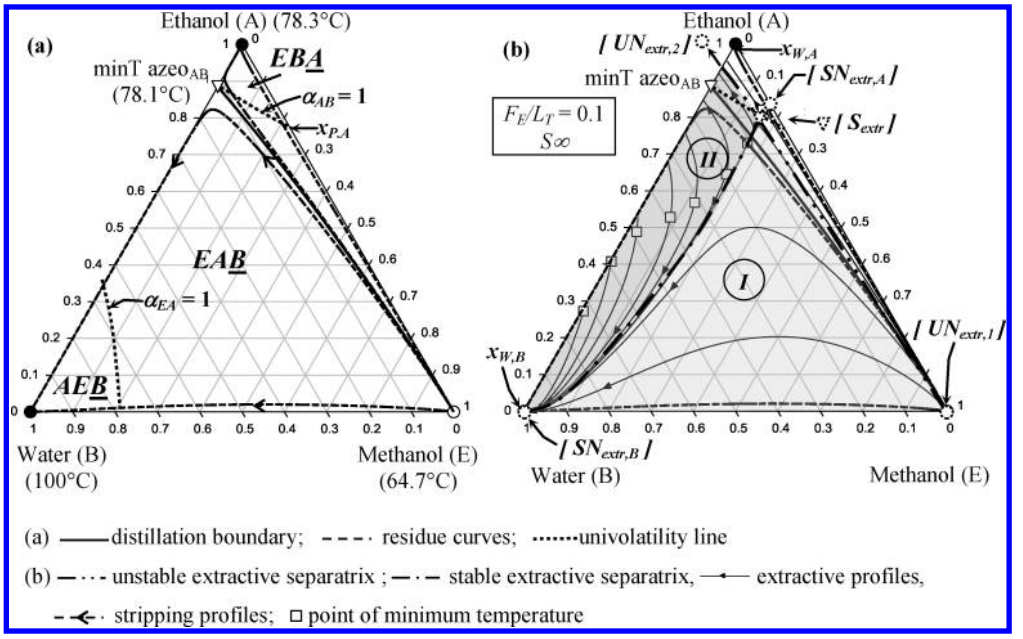

Figure 4. (a) Ethanol (A)−water (B) with methanol (E) 1.0−2 residue curve map with unidistribution and univolatility lines and (b) extractive profile maps at $F_E/L_T = 0.1$, $x_{W,B} = 0.99$, and an infinite reboil ratio.

batch extractive stripping column under an infinite reboil ratio in regions AEB and EAB on each side of the univolatility curve $\alpha_{EA} = 1$. Also, ethanol (A) can be recovered in the small region EBA above $\alpha_{AB} = 1$ for $(F_E/L_T) < (F_E/L_T)_{max,A}$. As x_{PA} is close to ethanol, $(F_E/L_T)_{max,A}$ is small (~0.13), and ethanol can be recovered in only a narrow operating range. When F_E/L_T varies, the detailed feasibility analysis under an infinite reboil ratio is similar to the 1.0−2 case in ref 10 for a maxT azeotrope extractive distillation with a heavy entrainer.

First, we consider a small value of $F_E/L_T = 0.1$ under total reboil $S = \infty$ (Figure 4b). Because $F_E/L_T < (F_E/L_T)_{max,A}$, the ternary extractive saddle point S_{extr} that was located at the minT azeo$_{AB}$ at $F_E \rightarrow 0^+$, moves inside the triangle along $\alpha_{AB} = 1$ and splits the composition space in four regions by extractive separatrices connecting four extractive nodes $SN_{extr,A}$, $SN_{extr,B}$, $UN_{extr,1}$ and $UN_{extr,2}$, that later being outside the composition triangle. Notice that the extractive process feasible regions AEB and EAB limited by the unstable extractive separatrix are larger than the azeotropic process feasible regions for B recovery, which is limited by the simple distillation boundary from E to the minT azeo$_{AB}$.

In region I on the right of the stable extractive separatrix, extractive composition profiles reach $SN_{extr,B}$ (Figure 4b), which connects to a stripping liquid profile (residue curves) running from E to B near to the edge (E−B). Temperature always increases along the extractive profile, as usual. However, in region II, liquid composition profiles of the extractive section have two ways for intercepting one residue curve finishing at B: (1) extractive liquid profiles running on the left and close to the stable extractive separatrix and reaching $SN_{extr,B}$, similar to the extractive profiles belonging to region I, and (2) extractive liquid profiles going toward the edge azeo$_{AB}$−B, where they intercept a residue curve originated at E, turning near azeo$_{AB}$ and following the distillation boundary to end at apex B. In case 2, the temperature along the extractive liquid profiles is nonmonotonic and there is a point of minimum temperature located between $SN_{extr,B}$ and the segment azeo$_{AB}$−B. These minimum-temperature points are indicated in Figure 4b as white squares.

This unexpected feature was corroborated by rigorous simulation using CHEMCAD.[16] Methanol was fed as a saturated liquid at tray $N_E = 18$ (simulation 1) or 23 (simulation 2) from the top of a 25-tray adiabatic column with negligible pressure drop and tray holdup. The initial charge was divided into two parts: 80 kmol for the top vessel (tray 1) and 20 kmol for the boiler (tray 25). The two vessels are considered as dynamic vessels connected to the column top and bottom, respectively. The holdup and composition of the top vessel are influenced by the incoming flow, V_E, coming from the top of the column and fixed flow, L_E, flowing toward the column first tray. In the case of the boiler, the liquid variation of the liquid holdup is determined by the heat duty (defining V_S) and by the liquid flow L_S leaving the bottom of the distillation column. Therefore, in the simulation and even in practice, extractive distillation in a batch stripper cannot be considered as the exact opposite of batch rectifier operation.

The simulation results are displayed in Figure 5. One might notice that the composition profiles and top-vessel trajectory are different between the simplified model and the rigorous simulation. Two reasons can be proposed: First, the equations of the simplified batch stripper model are written as the inverse operation of a rectifying column with a constant reboil ratio. However, as stated earlier, this is not true with rigorous simulation and in practice. Second, rigorous simulation includes the energy balance, and the feeding of the saturated liquid entrainer at the middle of the column affects the liquid flow rate going down the column and the vapor flow rate going up as well. Consequently, a batch stripper column allows the accumulation of water in the dynamic boiler, whereas water is depleted inside the top dynamic vessel. The boiler is considered as a vapor−liquid flash drum at given heat duty (Q_S), changing V_S on time. Therefore, V_S is not determined by S. Indeed, the theoretical reflux ratio in the bottom of the column can be considered as $V_S/(L_S - V_S)$, and it will not be constant during the process. In contrast, in the

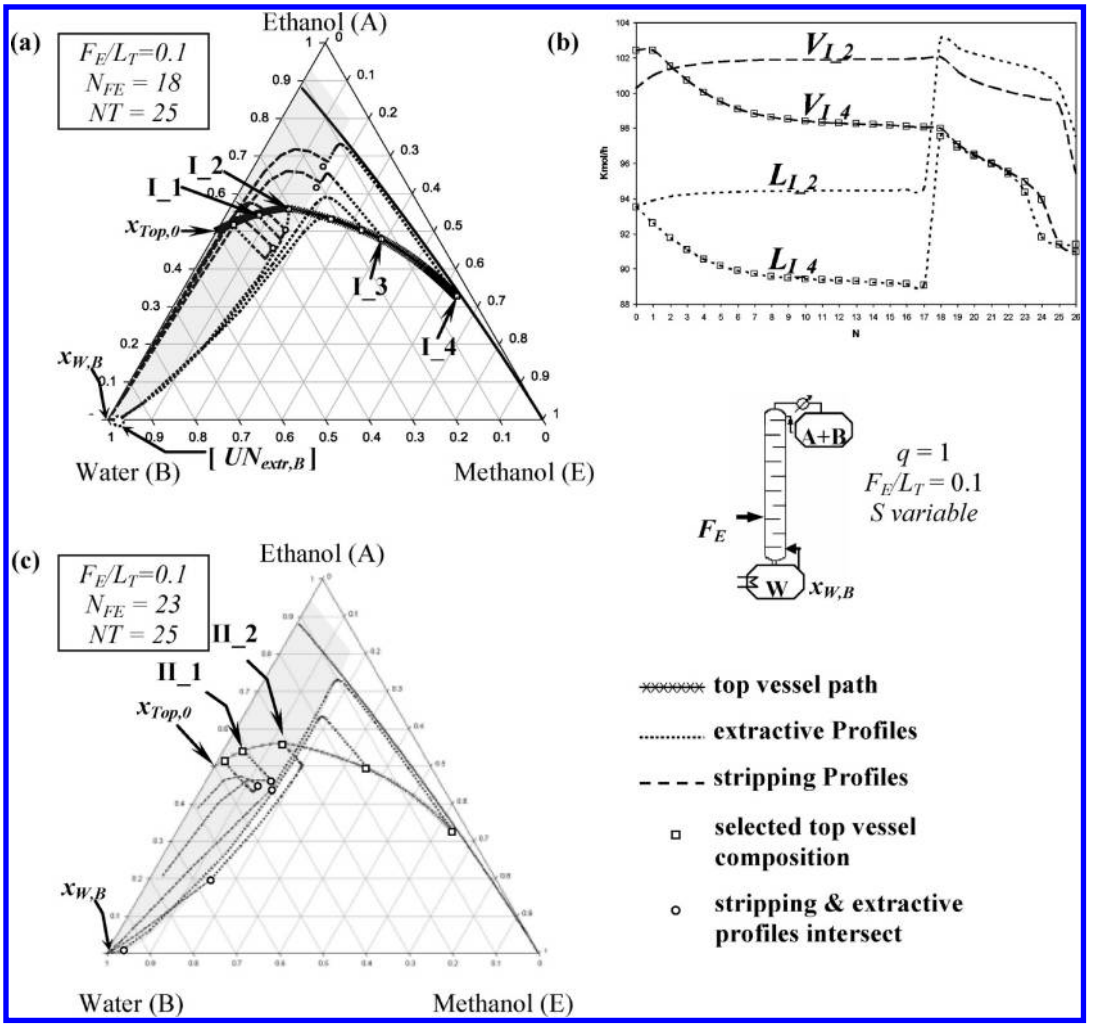

Figure 5. Simulation of ethanol−water batch extractive stripping using methanol as the light entrainer. Simulation 1: q = 1, F_E/L_T = 0.1, S variable, N_E variable, and $x_{Top,0}$ variable.

simplified model of the batch stripper, the extractive liquid profiles are computed with a constant S (eqs 8−11).

Simulation 1 (Figure 5a,b) corresponds to an equimolar ethanol−water initial charge ($x_{Top,0}$ in region II) distributed between the top vessel (80 mol) and the boiler vessel (20 mol). The methanol (F_{EL}) and the liquid flow rates coming from the top vessel (L_T) are defined to set an average ratio F_{EL}/L_T = 0.1 inside the extractive section. The extractive operation proceeds in two steps. In the first step, the heat duty (Q_{S1} and thus V_{S1}) is set to achieve $x_{W,water}$ > 0.99 into the boiler liquid holdup, which amounts to approximatively 20 mol. In the second step, accumulation of water in the boiler is achieved by defining a lower heat duty ($V_{S2} < V_{S1}$). Step 2 ends when x_{Top} no longer changes. Setting a correct V_S value is tricky because it is correlated with the L_T value. If V_S is very low, contamination of the still content occurs very quickly with ethanol and methanol. If V_S is too high, the boiler dries up.

Figure 5a displays the liquid composition trajectory inside the top vessel during steps 1 and 2. Direction is set by the feeding of methanol ($+x_E$) and by the transfer of water from the top vessel toward the boiler ($-x_{Top}$) to achieve $x_{W,water}$ > 0.99 at the end of step 1. During step 1, as x_{Top} remains in region II (shaded area taken from Figure 4), the extractive and stripping profiles intersect (white circles) at the minimum-temperature position inside the column (see point I_1 in Figure 5a). Because of the feeding of the cooled entrainer at this tray, it has the lowest temperature of the column. However, as the extractive process continues, the composition of methanol increases in the extractive section of the column and also in the top vessel. The composition trajectory of the top vessel then leaves the region II (point I_2 in Figure 5a) and enters region I. Then, the temperature of the tray where the entrainer is fed is no longer a minimum, and the whole column liquid profile follows an increasing temperature direction from the top (x_{Top}) to the boiler (x_W). Also, at point I_2, the boiler main impurity is methanol because the stripping profile nears the water−methanol edge. Later, at point I_3 (Figure 5a), the main impurity in the boiler is again ethanol because the stripping profile shifts back to region II on the water−ethanol edge and stays there until the end of the process (point I_4). For points I_3 and I_4, the temperature profile is monotonically increasing because x_{Top} lies inside region II where the light methanol composition is important. Notice that, during the whole operation, the extractive and stripping profiles always intersect close to the unstable extractive separatrix (see right edge of the shaded area in Figure 5a) when B is reached through the A−B edge instead of the B−E edge.

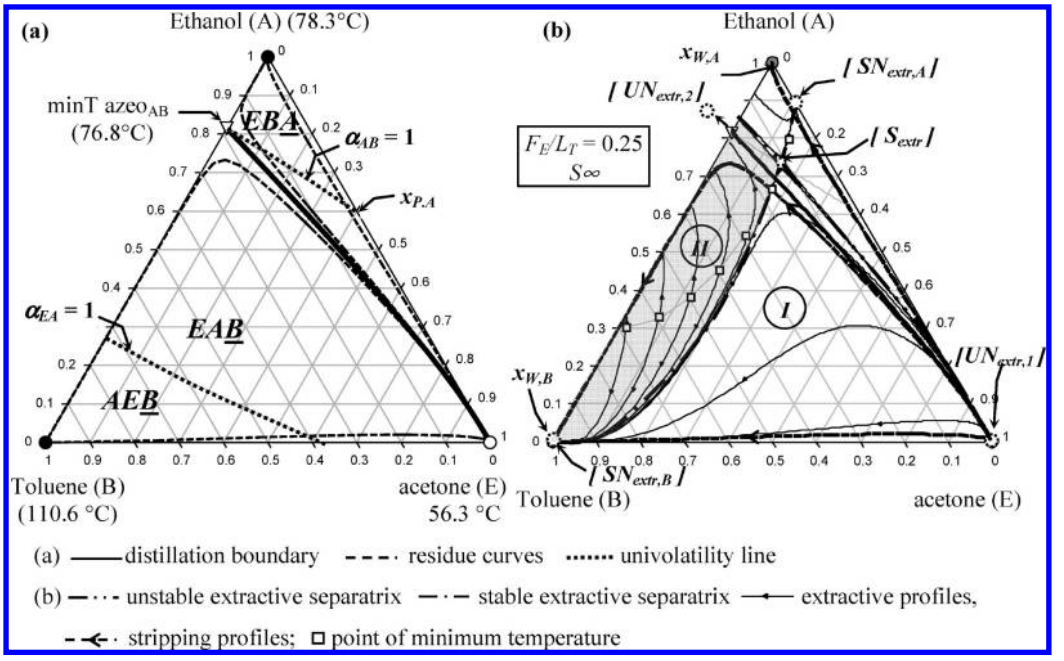

Figure 6. (a) Ethanol (A)−toluene (B) with acetone (E) 1.0−2 residue curve map with unidistribution and univolatility lines and (b) extractive profile map at $F_E/L_T = 0.25 < (F_E/L_T)_{max,B}$, $x_{W,B} = 0.99$, and and infinite reboil ratio.

The reboil ratio S increases during step 2. Indeed, the liquid L and vapor V flow rates along the column at the end of step 1 (1.25 h, point I_2) and step 2 (point I_4) (Figure 5b) are not constant along the column. Because of the effects of the inclusion of the energy balance and the entrainer feed state, differences between vapor and liquid flow rate are higher into the extractive section than stripping section. In fact, for point I_4, the liquid and vapor flow rates are almost identical in the stripping section (trays 19−27), and the column works almost under an infinite reboil ratio, prompting us to stop the simulation after 10.4 h of operation. $x_{W,water}$ reached a molar composition of 0.9956 in the boiler, and recovery equaled 87%. Similar results were achieved using a BatchColumn column: the liquid profiles varied at approximately the same operating time. Only the water recovery yield was higher at 93.8% (0.9982 of molar purity).

For simulation 2 (Figure 5c), methanol was fed at tray $N_E = 23$ as a boiling liquid, increasing the extractive section to the detriment of the stripping section (only two trays). Keeping the same operating times and stopping criterion as in simulation 1, the top-vessel composition trajectory is very similar to that in Figure 5a, but the liquid profiles are different inside each section. At the beginning of step 1, the stripping section is too short to reach the desired purity x_{WB}. Nevertheless, the extractive liquid profiles have the same shapes as in the previous case because of the small composition of methanol inside the column. The entrainer feeding tray retains the lowest temperature in the column. Then, after point II_2, the extractive section and the top vessel become richer in methanol and shift into region I: the stripping profile reaches the water vertex from the methanol−water edge passing through $SN_{exrtr,B}$. Because of the small number of trays into the stripping section, the water apex is always reached by liquid profiles running close to the E−B edge during the whole process. The water molar purity (0.9942) and recovery yield (87.1%) are similar to those obtained in simulation 1.

In the literature, Laroche et al.[5] used a sequence of two continuous azeotropic distillation columns to separate ethanol and water. Water was recovered from a 90-equilibrium-tray distillation column where methanol was fed along with the main azeotropic feed at tray 20 from the bottom of the column. The stripping liquid profile was located near the ethanol−water azeotropic edge as well. Compared with our extractive process, a large amount of methanol had to be fed with the main feed $F_E/F_{azeo} = 7$ and a very high bottom reflux ratio was used ($S = 218$). Separation of isopropanol−toluene using acetone was another example studied, requiring a total number of trays of 62, with entrainer fed at tray 10, $F_E/F_{azeot} = 10$, and $S = 127$. Again, the stripping liquid profiles were located near the azeotropic edge.

5.2. Ethanol (A)−Toluene (B) minT Azeotrope with Acetone (E). $\alpha_{AB} = 1$ Intercepts the A−E Edge. The separation of the ethanol (78.3 °C)−toluene (110.6 °C) minimum-boiling azeotrope (76.8 °C at $x_{ethanol} = 0.82$) with acetone (56.3 °C) is similar to that of the previous mixture, as $\alpha_{AB} = 1$ also intercepts the A−E edge. Now, however, we investigate the recovery of A as well as B. Figure 6a shows that the volatility order region EBA to recover ethanol (A) is greater than for the previous ethanol−water−methanol mixture (Figure 4a).

Figure 6b displays the extractive liquid profiles map for $F_E/L_T = 0.25$ at $S = \infty$ for recovering B. As expected, when $F_E/L_T = 0.25 < (F_E/L_T)_{maxA}$ (~0.40), five extractive singular points exist: located on the univolatility line $\alpha_{AB} = 1$, a ternary extracted saddle S_{etxr} connects four nodes $UN_{extr,1}$, $UN_{extr,2}$, $SN_{extr,B}$, and $SN_{extr,A}$ and divides the triangle into four extractive distillation regions. Above and below the unstable extractive separatrix, the extractive profiles end at either $SN_{extr,A}$ or $SN_{extr,B}$, where they can intersect a stripping profile, reaching either $x_{W,A}$ (ethanol) or $x_{W,B}$ (toluene), respectively. As in Figure 4b, when toluene (B) is sought as bottom product, the stripping profile can follow either a path along the E−B edge while x_{Top} lies inside region I with an ever-increasing temperature in the column or one near the {azeo$_{AB}$−B} segment if x_{Top} lies in region II, likely with a point of minimum temperature in the column.

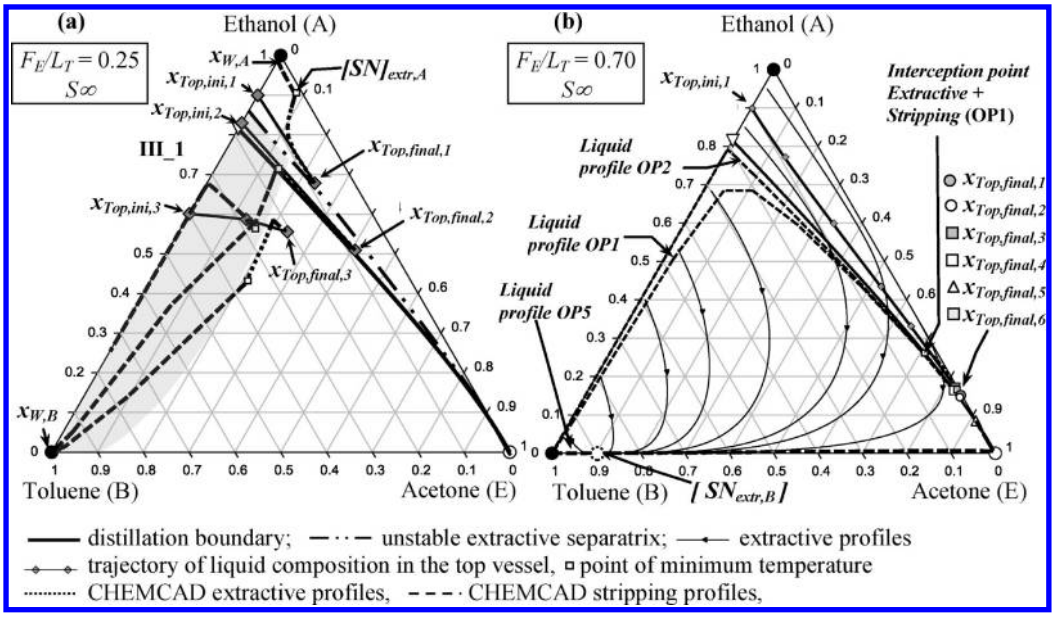

Figure 7. Simulation of batch extractive stripping of ethanol−toluene with acetone using CHEMCAD for several initial compositions of the binary mixture in the top vessel.

Rigorous simulation of extractive stripping was performed with CHEMCAD, with the same column features as for the previous mixture methanol−ethanol−water. Three initial feeds were considered: $x_{Top,ini,1}$ located above the stable extractive separatrix, $x_{Top,ini,2}$ located below the distillation boundary, and $x_{Top,ini,3}$ placed between the two boundaries (see Figure 7a). Simulation is only presented for operating step 1. The heat duty was set to maintain the boiler holdup approximately constant to achieve either $x_{W,A}$ or $x_{W,B} = 0.99$ in the boiler.

Starting from $x_{Top,ini,1}$, the extractive liquid profile for point $x_{Top,final,1}$ goes to $SN_{extr,A}$ on the acetone−ethanol edge, where it connects with the stripping profile ending at the ethanol vertex, which is the product $x_{W,A}$. Starting from $x_{Top,ini,2}$ between the two stable extractive separatrix and the distillation boundary of the residue curve map, the extractive liquid profile for point $x_{Top,final,2}$ intercepts a stripping profile (open square in Figure 7a) ending at the toluene (B) vertex, which is the product $x_{W,B}$. In this case, azeotropic distillation in a batch stripper with all of the acetone added to the initial charge of the top vessel would also enable the recovery of A, because $x_{Top,final,2}$ is located in the region in which A is the stable node SN_{rcm} of this distillation region. In that case, a single stripping profile would exist in the column running near the simple distillation boundary from $x_{Top,final,1}$ or $x_{Top,final,2}$ to the ethanol apex.

Starting from $x_{Top,ini,3}$, the same behavior as for the ethanol−water−methanol case is observed. The $x_{Top,3}$ trajectory is influenced by the feeding of acetone ($+x_E$) and the depletion of toluene ($-x_{W,B}$) because B moves toward the boiler to get accumulated. Whereas the top-vessel composition lies inside region II (point III_1 in Figure 7), the extractive and stripping profiles intersect at a point of minimum temperature (open square in Figure 7). When $x_{Top,3}$ lies in region I after crossing the stable extractive separatrix, the temperature profile is monotonically increasing (shown for $x_{Top,final,3}$ in Figure 7). Similar simulation results were obtained using BatchColumn software, setting the vapor flow rate leaving the boiler in accordance with the heat duty set in CHEMCAD.

When F_E/L_T is further increased under an infinite reboil ratio, S_{extr} moves on the univolatility line $\alpha_{AB} = 1$ until it reaches the E−A edge at $x_{P,A}$ for $(F_E/L_T)_{max,A}$. As seen in Figure 7b for $F_E/L_T = 0.7$, above $(F_E/L_T)_{max,A}$, neither $SN_{extr,A}$ nor the unstable extractive separatrix exist. Then, all extractive profiles computed by the simplified model reach the unstable node $SN_{extr,B}$, and B is the only possible product, for any composition. Starting from $x_{Top,ini,1}$, six operating cases were investigated by simulation with CHEMCAD to check the influence of the entrainer feed physical state, either boiling liquid (OP1) or saturated vapor (OP3, OP4), the position of the entrainer feed (OP2), the split of the initial charge between the top vessel and the boiler (OP5), and the entrainer feed ratio (OP6). The total number of trays, N_T, was reduced from 25 to 15 as this maintained the purity but reduced the total time. The molar purity of toluene in the still at the end of the process was fixed at 0.99 along with a recovery yield of 90%.

- (OP1) Acetone was fed as a saturated liquid at $N_{FE} = 10$, $F_E/L_T = 0.7$, $[V_S/(F_E + L_T)] \approx 0.88$. The 100 kmol initial charge was split in half between the boiler and the top vessel. The total operating time was 9.8 h with a consumption of entrainer/initial charge equal to 6.4. The top-vessel composition trajectory always remained above the distillation boundary of the residue curve (Figure 7b). The shape of the liquid profile at the end of the process ($x_{Topfinal,1}$) matched that reported in Figure 5c for the mixture methanol−ethanol−water. Notice that the initial charge into the boiler (50 kmol) was higher than the total amount of toluene that could be recovered (10 kmol). Therefore, to obtain only pure toluene at the end in the boiler, more mixture would have to be vaporized by defining $V_S > L_S$. Hence, the V_S value had to be selected carefully to avoid the contamination of the still with acetone while the ethanol goes at the top and the toluene concentrates into the boiler.
- (OP2) The same conditions as for OP1 were applied, except that acetone was fed at the top of the column. The computed operating time was slightly higher (10.2 h), while $V_S/(F_E + L_T)$ was kept constant to achieve a similar purity

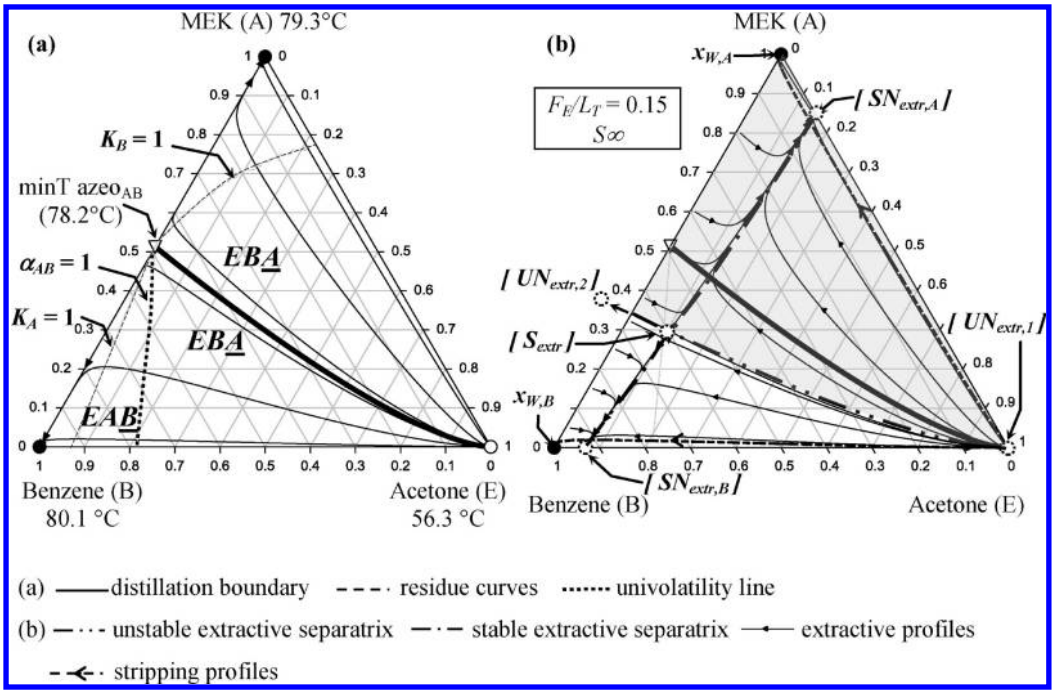

Figure 8. (a) MEK (A)−benzene (B) with acetone (E) 1.0−2 residue curve map with unidistribution and univolatility lines and (b) extractive profile map at $F_E/L_T = 0.15 < (F_E/L_T)_{max,B}$, $x_{W,B} = 0.99$, and an infinite reboil ratio.

and recovery yield of toluene. The final top-vessel composition ($x_{Topfinal,2}$) was near the distillation boundary, and the final liquid composition profile looked like a residue curve passing very near the distillation boundary. That was expected because the column had no extractive section, but a stripping section, whose profile usually matches a residue curve. Otherwise, the results were similar to OP1 with a simpler operating path.

- (OP3) The same conditions as for OP1 were applied, but considering the feeding of acetone as a saturated vapor. The V_S flow rate had to be adjusted at $V_S/(F_E + L_T) \approx 0.47$. The total operating time was slightly shorter than for OP1 (8.5 h), whereas the top-vessel trajectory and the final liquid profile inside the column (at $x_{Topfinal,3}$) were almost identical to case OP1.
- (OP4) The same conditions as for OP2 were applied, but considering the feeding of acetone as a saturated vapor. The V_S flow rate also had to be adjusted at $V_S/(F_E + L_T) \approx 0.48$, very similar to the previous case (OP3). The total operating time was close to that of case OP3 (8.8 h), and the top-vessel trajectory and final liquid profile composition (at $x_{Topfinal,4}$) were very similar to those of case OP2.
- (OP5) The same conditions as for OP1 were applied, but the initial charge was distributed as 5 kmol in the boiler and 95 kmol in the top vessel. The initial heat duty fixed in the boiler was slightly smaller than that in case OP1, more like a typical stripper, facilitating $V_S < L_S$. Keeping V_S constant, during the first one-third of the process duration, all three components accumulated in the boiler until the liquid total amount reached a maximum value of around 40 mol, which corresponded to $V_S \approx L_S$. After that, $V_S > L_S$, the boiler steadily depleted until toluene remained with a molar purity was 0.99, and the recovery yield was 90%. The whole process was 1.9 times longer than case OP1 and consumed much more entrainer. The final top-vessel composition ($x_{Topfinal,4}$) lay on the distillation boundary, close to the acetone apex. In this case, the liquid profile into the column reaches the toluene vertex passing by the acetone apex and running on the edge acetone−toluene as predicted by the simplified modeling.
- (OP6) Similar to case OP1, but the ratio $F_E/L_T = 0.5$ was reduced. The total operating time increased by 1.26 times. However, the consumption of entrainer versus initial charge droped from 6.4 to 5.7.

BatchColumn simulations gave a similar trend but computed a slightly greater operating time.

In conclusion, operating alternatives given by OP1 and OP3 are the simplest operating modes and provide the best simulation results to separate toluene by using two dynamic vessels with a substantial liquid amount, connected to an extractive distillation column. The feeding of the entrainer as a saturated vapor brings more complication than the gain in total operating time. The initial binary mixture had a low composition of toluene, which increased its recovery and explained the large entrainer consumption and operating time. In all cases, the V_S value was strongly related to L_T and F_E, and it had to be selected carefully to obtain the desired recovery yield and purity of toluene.

5.3. Methyl Ethyl Ketone (A)−Benzene (B) minT Azeotrope with Acetone (E). $\alpha_{AB} = 1$ Intercepts the B−E Edge. The separation of the methyl ethyl ketone (79.3 °C)−benzene (80.1 °C) minimum-boiling azeotrope (78.2 °C at x_{MEK} = 0.51) with acetone (56.3 °C) belongs to class 1.0−2 with a univolatility curve $\alpha_{AB} = 1$ that reaches the B−E edge (Figure 8a). Therefore, extractive distillation in a stripper configuration should now favor the recovery of A instead of B, as before. For a batch azeotropic stripping process, the simple distillation boundary is slightly curved, and MEK (A) is placed on the concave side, enabling its removal as a bottom product but with a recovery that is not very good because the distillation boundary is

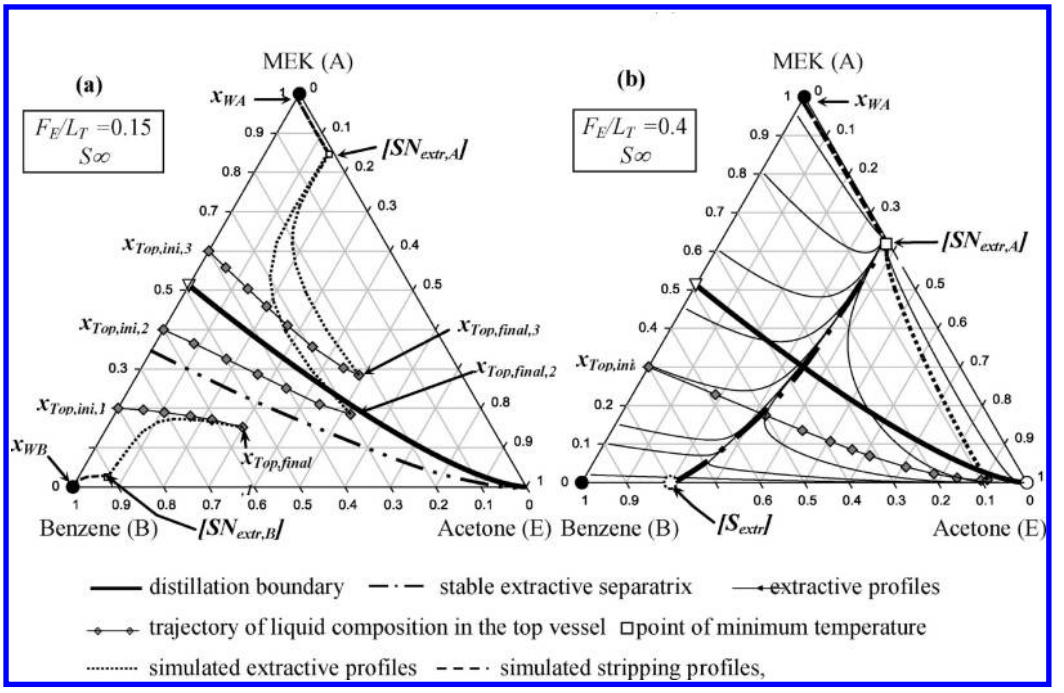

Figure 9. Simulations of batch extractive stripping of MEK−benzene with acetone using (a) BatchColumn and (b) CHEMCAD for F_E/L_T (a) below and (b) above $(F_E/L_T)_{max,B}$ and various initial compositions.

not close enough to the E−B edge. A batch extractive stripper alternative can improve recovery because the extractive feasible region EBA is much greater than the simple distillation region defined by the distillation boundary of the residue curve map, a behavior similar to that of the previously studied mixtures. Finally, there exists a maximum $(F_E/L_T)_{max,B}$ to obtain product B under an infinite reboil ratio if the top-vessel composition lies in the volatility order region EAB.

Figure 8b displays the map of extractive profiles at F_E/L_T = 0.15 < F_{maxB}. Again, the ternary extractive saddle S_{extr} located on the univolatility line is connected to two unstable extractive nodes ($UN_{extr,1}$, $UN_{extr,2}$) and two stable extractive nodes ($SN_{extr,A}$, $SN_{extr,B}$). A composition inside the two shaded regions above the unstable extractive separatrix allows recovery of MEK in the boiler. Outside this region, benzene is the bottom product. Note that, even for $F_E/L_T < (F_E/L_T)_{max,B}$, the feasible region for separating MEK (A) by extractive distillation is much greater than that for azeotropic distillation, set by the distillation boundary of the residue curve map.

To validate the ability of the general criterion to predict which product can be recovered depending on the volatility order region (Figure 8b), rigorous simulations were run using BatchColumn software (Figure 9). Three binary mixture initial compositions were considered: $x_{Top,ini,1}$ below the stable extractive separatrix, $x_{Top,ini,2}$ between the stable extractive separatrix and the distillation boundary, and $x_{Top,ini,3}$ above the distillation boundary. In all cases, the initial charge to the boiler was 20 kmol and F_E/L_T = 0.15 at total reflux. For composition $x_{Top,ini,1}$, located in the volatility order region EAB, a column with N_T = 25 and N_{FE} = 18 enabled recovery of benzene (B) (Figure 9a). For composition $x_{Top,ini,2}$, located in the volatility order region EBA, a column with N_T = 40 and N_{FE} = 28 enabled recovery of MEK (A). Notice that an azeotropic process would have recovered benzene because $x_{Top,ini,2}$ is located below the distillation boundary where benzene is SN_{rcm}. For the composition $x_{Top,ini,3}$ located in the volatility order region EBA, MEK (A) is again recovered by extractive distillation (and also by azeotropic distillation as it is above the distillation boundary).

Comparing the simplified modeling (Figure 8b) and rigorous simulation results (Figure 9a), the liquid profiles match very well. Intersection between the rigorous extractive and stripping section liquid profiles takes place very close to the theoretical $SN_{extr,A}$ or $SN_{extr,B}$, depending on the case.

As F_E/L_T increases, the ternary extractive saddle S_{extr} moves along the univolatility line α_{AB} = 1 toward the acetone−MEK edge. For F_E/L_T = 0.4 > $(F_E/L_T)_{max,B}$ (~0.38), the unstable extractive separatrix disappeared, and $SN_{exts,B}$ merged with S_{extr} (Figure 9b). Then, all extractive profiles reached the unique unstable extractive node $SN_{extr,A}$, and only MEK (A) could be recovered by extractive distillation under an infinite reboil ratio. This behavior was confirmed by rigorous simulation with CHEMCAD using the same operating conditions as in Figure 9a and starting from $x_{Top,ini}$ = 0.3, that is, in the region where benzene (B) was obtained for F_E/L_T = 0.15 (Figure 9a). Now, for F_E/L_T = 0.4, MEK (A) was recovered with a molar composition of 0.99 and a 68% recovery yield after 20 h of operating time. Through the heat duty, V_S was defined to obtain the largest amount of MEK in the bottom vessel at the end of the process. Therefore, a progressive increasing of concentration of MEK in the bottom vessel took place during the extractive distillation process. The feeding of acetone as a saturated vapor gave similar results.

A similar example was discussed by Laroche et al. for the separation of ethyl acetate (A) (77.1 °C)−ethanol (B) (78.4 °C) using acetone (E) as a light entrainer in a sequence of two continuous distillation columns.[5] The extractive column had 91 equilibrium trays with methanol being fed in tray 22 near the bottom along with the main azeotropic mixture. Separation of ethyl acetate (A) as the bottom product in the extractive column was achieved using F_E/L_T = 30 and a very high bottom reflux

ratio (S = 126). Ethanol was the bottom product of the second distillation column.

To summarize this section, the general feasibility criterion for the separation of minimum-boiling azeotropic mixtures using light entrainers (1.0−2 diagram) is satisfied for both original components A and B but depends on the location of the univolatility line α_{AB}, which sets limiting values for the entrainer feed flow rate F_E/L_T for one of the products. In addition, the extractive distillation process offers a larger feasible region than the azeotropic distillation process.

6. SEPARATION OF MAXIMUM-BOILING-TEMPERATURE AZEOTROPES WITH LIGHT ENTRAINERS (1.0−1A CLASS)

The separation of a maximum-boiling azeotropic mixture using a light entrainer corresponds to the ternary diagram 1.0−1a, the opposite of the separation of a minimum-boiling azeotrope using a heavy entrainer.[3] The topological and thermodynamic characteristics of the extractive profile map when varying the entrainer flow rate and the reflux ratio were fully detailed in the first part of this series of articles.[10]

For the present case with a light entrainer, separation of azeotropic component A or B is not possible using azeotropic distillation with the entrainer fully added with the mixture because the two are saddle points and are located in different batch distillation regions. However, the separation can be achieved by extractive distillation when the light entrainer is fed at an intermediate tray of the batch column, giving rise to an extractive section and a stripping section. Application of the general feasibility criterion under an infinite reboil ratio indicates that, depending on the intercept of the univolatility curve α_{AB} with the triangle, say, the B−E edge (A−E edge), component B (A) is withdrawn as the product from the column bottom. However, this can be accomplished only above a minimum value of $(F_E/L_T)_{min,B}$ $[(F_E/L_T)_{min,A}]$, so that the ending point of the extractive profiles $SN_{extr,B}$ ($SN_{extr,A}$) is near the B−E edge (A−E edge) and can intersect a stripping profile, similar to a residue curve, that reaches the product B (A) (see Figure 3c,d).[10]

6.1. Water (A)−Ethylenediamine (B) maxT Azeotrope with Methanol (E). α_{AB} = 1 Intercepts the B−E Edge. The separation of the water (100 °C)−ethylenediamine EDA (117.1 °C) maximum-boiling azeotrope (120.0 °C at x_{water} = 0.40) with methanol (64.5 °C) belongs to class 1.0−1a with a univolatility curve α_{AB} = 1 that reaches the B−E edge (Figure 10) and is the unique example studied in the literature by using extractive distillation process, considering a rectifying[19] or a stripper[22] column configuration.

Then, the importance of the univolatility line was not understood, and the feasibility analysis relied on the tedious computing of extractive and rectifying (or stripping) profiles under several operating conditions and strategies for feeding the light entrainer at different positions of the distillation column.

Here, EDA (B) fulfils the general feasibility criterion and can be drawn as the first bottom product. In Figure 11a, for F_E/L_T = 0.5 below $(F_E/L_T)_{min}$ (~0.62), the ending point of all extractive profiles $SN_{extr,B}$ lies on the univolatility line and therefore cannot intersect the residue curve computed from x_{WB} = 0.98 that represents the liquid profile inside the stripping section at infinite reboil ratio. Two binary extractive saddles $S_{extr,A}$ and $S_{extr,B}$ coming from the methanol and EDA apices also exist. For $F_E/L_T = 1 > (F_E/L_T)_{min}$, $S_{extr,B}$ merges into $SN_{extr,B}$, which now lies

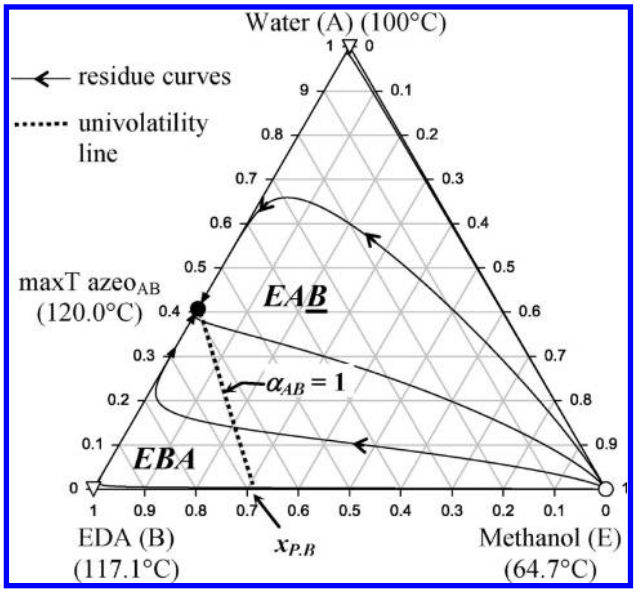

Figure 10. Water (A)−ethylenediamine (B) with methanol (E) 1.0−1a residue curve map and univolatility line.

near the B−E edge and can intersect a stripping profile reaching x_{WB}. The whole diagram is feasible. When a finite reboil ratio is set, an unfeasible region occurs (Figure 11b) and is limited by an unstable extractive separatrix. This is much like what was observed for the opposite case of a minT azeotrope separation with a heavy entrainer where an unstable extractive separatrix prevented the total recovery of the product in the distillate.[10]

Varga[22] did a rigorous simulation using BatchColumn for a stripper with 40 theoretical plates and methanol fed at plate four above the boiler, which enabled the separation of 130 kmol of azeotropic mixture water−EDA with methanol. The whole azeotropic mixture was initially loaded into the top vessel (7 L), and the column plates (0.05 L) were filled with pure entrainer, including the boiler (0.1 L). F_E/L_T was set equal to 2 and $S \approx 55$. After 10 h, 95 molar % EDA was obtained, with a final recovery of 80%. Methanol was the main impurity. As expected under a finite reboil ratio, the process had to be stopped because the top-vessel composition entered the unfeasible region. Again, the methanol consumption was very high, as indicated by the top-vessel path that goes toward the methanol apex. Figure 11b displays the results of Varga,[22] namely, the top-vessel path and the column profile in both the extractive and stripping section after 3 h, along with the extractive profile map computed by the simple model.

6.2. Chloroform (A)−Acetone (B) maxT Azeotrope with Dichloromethane (E) and Methyl Isobutyl Ketone (A)−Propanoic Acid (B) maxT Azeotrope with Dimethylformamide (E). α_{AB} = 1 Intercepts the A−E Edge. Feasibility analysis when the univolatility line intersects the A−E edge has not yet been published in the literature. As the opposite case of separation a minimum-boiling azeotropic mixture using a heavy entrainer where the heavy azeotropic component (B) is drawn as first distillate product,[10] the light azeotropic component (A) then has to be pushed toward the column bottom. Therefore, the appropriate entrainer has to decrease the relative volatility between A and B, which is not the typical behavior sought by engineers. It is allowed if light E exhibits no deviation or a

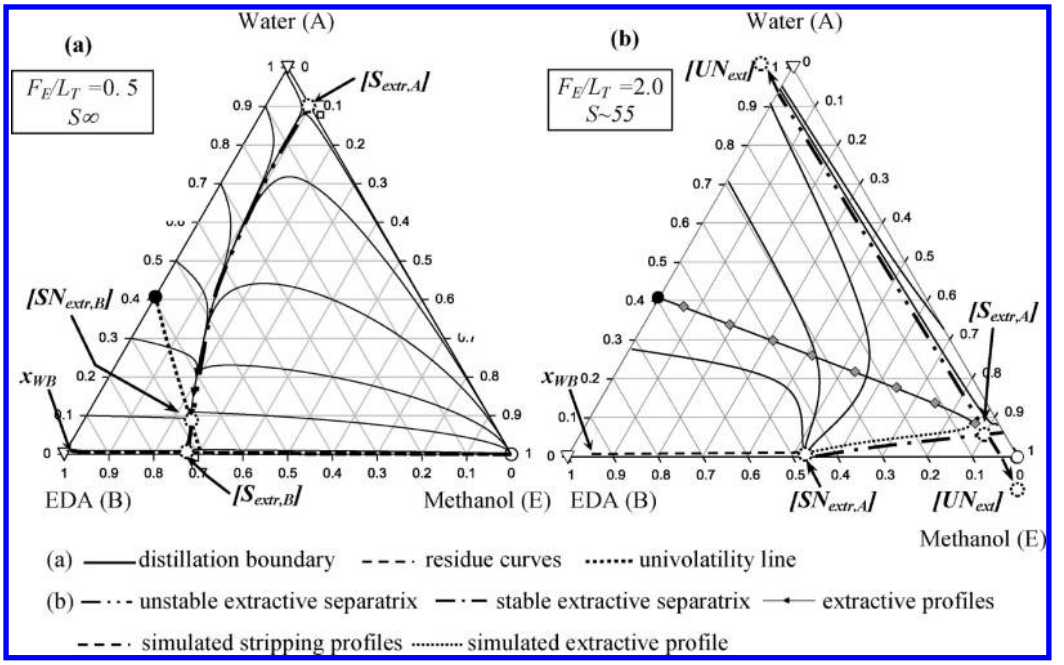

Figure 11. Water (A)−ethylenediamine (B) with methanol (E) extractive profiles map at F_E/L_T (a) below and (b) above $(F_E/L_T)_{min,B}$. (Part b adapted from results in ref 22.)

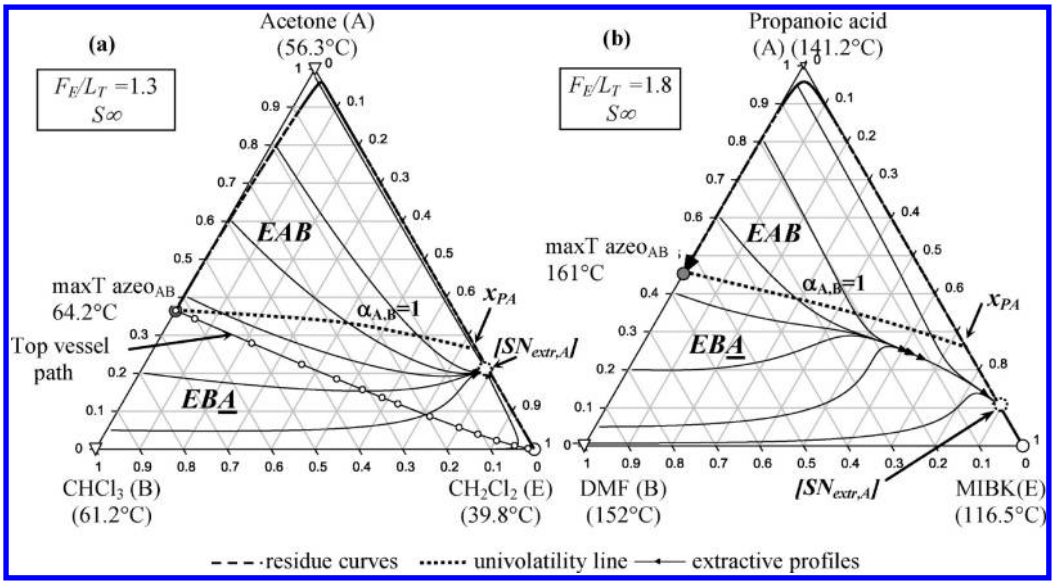

Figure 12. (a) Acetone (A)−$CHCl_3$ (B) with CH_2Cl_2 (E) and (b) propanoic acid (A)−DMF (B) with MIBK (E) 1.0−1a residue curve maps, univolatility lines, and extractive profile maps for $F_E/L_T > (F_E/L_T)_{min,A}$.

negative deviation of Raoult's law with A and a positive deviation or no deviation with B. Such a mixture can be found in which A is a carboxylic acid or a chloride.

After extensive searching among ternary mixtures using the UNIFAC modified Dortmund 1993 model, we considered the separation of the acetone (56.3 °C)−chloroform (61.2 °C) maximum-boiling azeotrope (64.2 °C at $x_{acetone}$ = 0.37) with dichloromethane (39.8 °C) and the separation of the propanoic acid (141.2 °C)−dimethylformamide (152 °C) maximum-boiling azeotrope (161 °C at $x_{prop\ acid}$ = 0.43) with methyl isobutyl ketone (MIBK) (116.5 °C). As displayed in Figure 12, both mixtures belong to class 1.0−1a with a univolatility curve $\alpha_{AB} = 1$ that reaches the A−E edge.

With this diagram configuration, the general feasible criterion under an infinite reboil ratio is satisfied for A, but a high consumption of the entrainer is expected because $x_{P,A}$ is near apex E. Indeed, both extractive section composition profile maps (Figure 12) show that the separation requires feeding of light entrainer as a saturated liquid above a minimum value $(F_E/L_T)_{min,A}$ determined by the point $x_{P,A}$ which is much larger than the previous examples in this article. Recall that, for $F_E/L_T < (F_E/L_T)_{min,A}$, the stable extractive node $SN_{extr,A}$ is located on the univolatility line, similar

to Figure 11a for the mixture methanol−water−EDA, and thus the extractive profile cannot reach a stripping profile reaching the expected product A.

For further validation, rigorous simulation using BatchColumn was performed for acetone−chloroform with dichloromethane considering a ratio of F_E/L_T = 1.3 and a closed operation with accumulation of the product in the still. The column had 20 trays, and CH_2Cl_2 was fed at the second plate. After 35 h of operation, the top vessel contained chloroform but also 98 mol % of entrainer (Figure 12a), whereas the product acetone had accumulated in the still, but was polluted with 82% of entrainer. A large consumption of 45 mol of dichloromethane per mole of azeotropic mixture was needed to recover 73% of acetone.

To summarize this section, the general feasibility criterion for the separation of maximum-boiling azeotropic mixtures using light entrainers (1.0−1a diagram) is satisfied for one original components, either A or B, depending on the location of the univolatility line α_{AB}, which sets minimum value for the entrainer feed flow rate F_E/L_T for one of the product. Entrainer consumption is also set by the univolatility line intersection.

7. SEPARATION OF LOW-RELATIVE-VOLATILITY MIXTURE WITH LIGHT ENTRAINERS (0.0−1 CLASS)

As mentioned in section 4, the separation of a low-α binary mixture by an extractive distillation process using a light entrainer has two subcases. In the most common subcase, the univolatility line α_{AB} does not exist, and component B is the product, as it is the least volatile in the whole composition triangle where a residue curve of decreasing temperature reaches the entrainer apex (Figure 3e). This was illustrated for the mixture chlorobenzene (A)−ethyl benzene (B) with 4-methylheptane (E) with rectifier[19] and stripper[22] configurations. When the univolatility line α_{AB} exists, it switches the A and B volatilities, and then the two components A and B are products in the EB$\underline{A}$ and EA$\underline{B}$ volatility order regions, respectively (Figure 3f). A requires a minimum entrainer flow rate ratio value $(F_E/L_T)_{min,A}$, much like the 1.0−1a case in section 6, whereas B recovery is limited by a maximum entrainer flow rate ratio value $(F_E/L_T)_{max,B}$, much like the 1.0−2 case in section 5.

For illustration, we consider the separation of the ethyl acetate (77.2 °C)−benzene (80.1 °C) low-relative-volatility mixture ($\overline{\alpha}_{AB}$ = 1.12) with acetone (56.3 °C). Figure 13 displays the thermodynamic features of the diagram.

The univolatility line α_{AB} intersects the A−E edge very close to the A apex at x_{PA} and the B−E edge also close to the B apex. Therefore, both $(F_E/L_T)_{min,A}$ and $(F_E/L_T)_{max,B}$ are moderate, suggesting an easier recovery of A for that mixture, as also hinted by the large EB$\underline{A}$ volatility order region. Location of the unidistribution line K_A = 1 near the A−B edge conducts residues curves to first reach the binary side AB before reaching the stable node B. Hence, separation of the stable component B by azeotropic distillation in a batch stripper as a bottom product and having a high purity will imply a high number of stages and a high reflux ratio because the average relative volatility is close to unity. For extractive distillation, separation of component A or B will depend of the selected value of F_E/L_T and the location of the initial charge of ethyl acetate−benzene in the ternary diagram.

Considering the isovolatility lines going from α_{AB} = 0.8 in the EB$\underline{A}$ region to α_{AB} = 1.1 in the EA$\underline{B}$ region, Figure 13 shows that acetone enhances the volatility of B more than that of A. This is why the univolatility line α_{AB} exists. However, the values are still

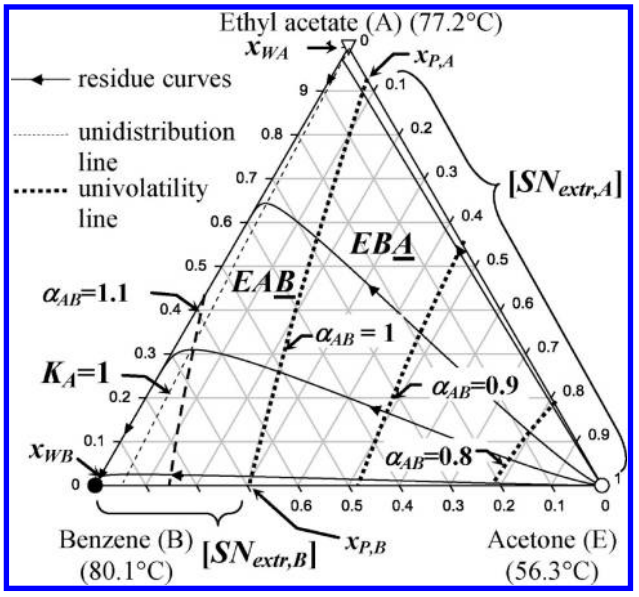

Figure 13. Ethyl acetate (A)−benzene (B) with acetone (E) 0.0−1 residue curve map and isovolatility lines.

close to unity, indicating that separation of A or B in a batch extractive stripper remains difficult in practice, requiring a high number of trays, reflux ratio, and operating time. However, this example remains an illustration of how the occurrence of the univolatility line α_{AB} can allow recovery of the saddle component A having an intermediate boiling temperature in the boiler instead of the heaviest component B.

First, we computed the map of extractive profiles under an infinite reboil ratio for $F_E/L_T = 0.1 < (F_E/L_T)_{min,A} < (F_E/L_T)_{max,B}$ (Figure 14a). As expected, the whole ternary diagram is feasible for the separation of benzene because all extractive profiles finish at $SN_{extr,B}$ located on the B−E edge, which can also cross a residue curve ending at the selected distillate composition (x_{WB}). There is a stable extractive separatrix linking the stable extractive node $SN_{extr,B}$ coming from apex B and the saddle extractive point S_{extr} originating from saddle vertex A. As benzene is also the stable node of the residue curve map, it goes to the column bottom at total reboil without or with light entrainer feeding. The feeding of acetone in extractive distillation affects only the liquid profile inside the column by providing a different thermodynamic path to link the composition in the top vessel and the composition in the boiler (x_{WB}) located around the benzene vertex.

A closed-operation BatchColumn simulation was performed with 50 theoretical plates and acetone fed at tray 10 above the boiler. A relation of F_E/L_T = 0.1 was defined. An equimolar mixture (100 kmol) of ethyl acetate−benzene (x_0) was initially split equally between the boiler and the top vessel, and a 0.99 molar composition in benzene was achieved in the boiler. Figure 14a shows the trajectory of the liquid composition in the top vessel and the liquid profile in the column at the end of the process (6 h). Notice the good agreement that exists between the liquid profiles computed by the simplified model and by the rigorous simulation.

Now, we consider F_E/L_T = 0.3, where $(F_E/L_T)_{min,A} < F_E/L_T < (F_E/L_T)_{max,B}$ (Figure 14b). Under these conditions, both A and B can be recovered. The ternary saddle point S_{extr} is located on the univolatility line at the crossing point of the two extractive separatrices. The unstable extractive separatrix splits the triangle into two regions. x_{S1} is located on the side in which the extractive

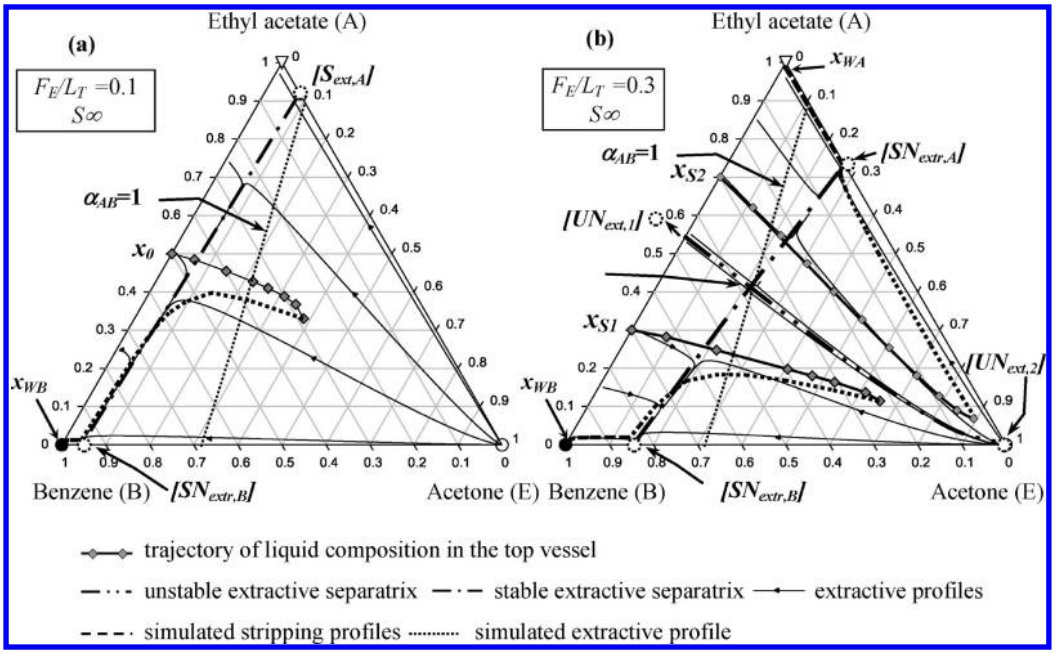

Figure 14. Extractive profile map and simulation results for the separation of ethyl acetate−benzene with acetone: (a) $F_E/L_T < (F_E/L_T)_{max,B}$ and (b) $(F_E/L_T)_{max,B} < F_E/L_T < (F_E/L_T)_{min,A}$.

section composition profiles reach $SN_{extr,B}$, enabling B to be obtained, and x_{S2} lies in the region where they reach $SN_{extr,A}$, to obtain A. Rigorous simulations with BatchColumn for both x_{S1} and x_{S2} confirmed those insights (Figure 14b): After 6 h, 9.7 kmol of 99 mol % benzene remained in the boiler from x_{S1} using the same column as earlier. From x_{S2} with acetone fed at tray six above the boiler, 34 h of operating time was required to obtain a mere 0.2 kmol of 99 mol % ethyl acetate into the still. For both cases, the number of trays in the stripping section was defined in order to deplete acetone before liquid profile reaches the boiler. Recovery of the saddle ethyl acetate in the bottom section was harder than separation of benzene, but still possible because of the existence of the univolatility line α_{AB}.

For $F_E/L_T = 0.5 > (F_E/L_T)_{max,B}$, only $SN_{extr,A}$ exists (Figure 15). Under an infinite reboil ratio, all extractive profiles finish at it and cross a stripping profile to obtain A in the boiler x_{WA}. As discussed in part 2[11] for the same separation of ethyl acetate−benzene but using *n*-butanol as a heavy entrainer, the size of the feasible region is quickly reduced under a finite reboil ratio, even at $S = 30$.

These simple model predictions were confirmed by rigorous simulation with CHEMCAD (Figure 15). Starting from an equimolar ethyl acetate−benzene mixture x_0, the feeding of acetone at tray 6 above the boiler (total tray number is 50) enabled the recovery of 99 mol % ethyl acetate in the boiler after 76 h, for $F_E/L_T = 0.5$. The boiler heat duty was set to be higher than 85% and to reach a recovery yield of 87.7%. The final ratio (entrainer amount)/(binary mixture amount) was large at ∼40 as indicated by the last composition, very close to the acetone vertex. Similar trajectory of the liquid composition in the top vessel and the liquid profile were obtained using BatchColumn software, but the total operating time for achieving the same recovery yield and purity was significantly higher.

To summarize this section, the general feasibility criterion for the separation of low-relative-volatility mixtures using light entrainers

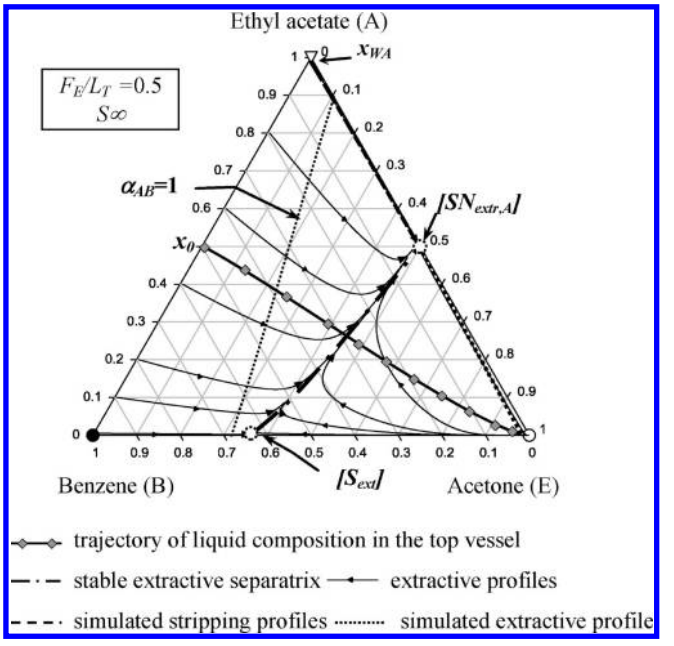

Figure 15. Extractive profile map and simulation results for the separation of ethyl acetate−benzene with acetone. $F_E/L_T > (F_E/L_T)_{max,B}$.

(0.0−1 diagram) depends on the existence of the univolatility line α_{AB}. When it does not exist, only B is a possible product. When it does, both original components A and B can be recovered, B below a maximum value of the entrainer feed flow rate F_E/L_T and A above a minimum value.

8. CONCLUSIONS

Separation of minimum- (1.0−2 Serafimov class) and maximum- (1.0−1a Serafimov class) boiling-temperature azeotropic

mixtures and of low-relative-volatility (0.0−1 Serafimov's class) mixtures A−B by batch extractive distillation using a light boiling entrainer E has been studied by several authors in a rectifying and stripping column configuration, where the latter is far more suitable. However, the literature works failed to understand the importance of the univolatility lines in multicomponent systems.

Considering the existence of the univolatility line α_{AB} and the thermodynamic features of the relevant mixtures, we have shown how, in accordance with the general extractive distillation feasibility criterion published in part 1,[10] thermodynamic insight alone can help assess the feasibility of the process, all possible products and also show whether limiting values exist for the key operating parameters, namely the entrainer flow rate and the reboil ratio.

For the separation of minimum-boiling azeotropic mixtures using light entrainers (1.0−2 diagram), both original components A and B satisfy the general feasibility criterion and can be recovered, depending on the location of the univolatility line α_{AB}, which sets limiting values for the entrainer feed flow rate F_E/L_T for one of the product. In addition, the extractive distillation process offers a larger feasible region than the azeotropic distillation process.

For the separation of maximum-boiling azeotropic mixtures using light entrainers (1.0−1a diagram) either A or B can be recovered, depending on the location of the univolatility line α_{AB}, that sets minimum value for the entrainer feed flow rate F_E/L_T for one of the product.

For the separation of low relative volatility mixtures using light entrainers (0.0−1 diagram), feasibility depends on the univolatility line α_{AB} existence. When it does not, B is the unique possible product. When it exists, both original components A and B can be recovered, B below a maximum value of the entrainer feed flow rate F_E/L_T and A above a minimum value.

All possible cases with the various locations of the univolatility line α_{AB} were illustrated with real mixtures, including some never published, such as the separation of a low-relative-volatility mixture with a light entrainer when a univolatility line α_{AB} exists. For validation, the thermodynamic insights were systematically checked by computing composition profiles with simple modeling and by running rigorous simulations.

Considering a light entrainer could now provide more opportunities to engineers aiming at the separation of minT and maxT azeotropic mixtures and low-relative-volatility mixtures. It was noticed during the simulations, however, that the batch process involves a large entrainer consumption, which might lower the benefit of the process gained from the use of a light-boiling entrainer, which is less energy demanding than that of a heavy boiler.

AUTHOR INFORMATION

Corresponding Author

*E-mail: Vincent.Gerbaud@ensiacet.fr.

ACKNOWLEDGMENT

The authors thank V. Varga, E. Rev, and Z. Lelkes for their discussions about the use of light entrainer in extractive distillation which initiated this work.

REFERENCES

(1) Doherty, M. F.; Caldarola, G. A. Design and synthesis of homogeneous azeotropic distillations. 3. The sequencing of columns for azeotropic and extractive distillations. *Ind. Eng. Chem. Fundam.* **1985**, *24* (4), 474–485.

(2) Kiva, V. N.; Hilmen, E. K.; Skogestad, S. Azeotropic Phase Equilibrium Diagrams: A Survey. *Chem. Eng. Sci.* **2003**, *58*, 1903–1953.

(3) Hilmen, E. K.; Kiva, V. N.; Skogestad, S. Topology of Ternary VLE Diagrams: Elementary Cells. *AIChE J.* **2002**, *48* (4), 752–759.

(4) Laroche, L.; Bekiaris, N.; Andersen, H. W.; Morari, M. Homogeneous Azeotropic Distillation: Comparing Entrainers. *Can. J. Chem. Eng.* **1991**, *69*, 1302–1319.

(5) Laroche, L.; Bekiaris, N.; Andersen, H. W.; Morari, M. The Curious Behavior of Homogeneous Azeotropic Distillation—Implications for Entrainer Selection. *AIChE J.* **1992**, *38*, 1309–1328.

(6) Steger, C.; Varga, V.; Horvath, L.; Rev, E.; Fonyo, Z.; Meyer, M.; Lelkes, Z. Feasibility of Extractive Distillation Process Variants in Batch Rectifier Column. *Chem. Eng. Process.* **2005**, *44*, 1237–1256.

(7) Brüggemann, S.; Marquardt, W. Shortcut Methods for Nonideal Multicomponent Distillation: 3. Extractive Distillation Columns. *AIChE J.* **2004**, *50*, 1129–1149.

(8) Levy, S. G.; Doherty, M. F. Design and synthesis of homogeneous azeotropic distillations. 4. Minimum reflux calculations for multiple-feed columns. *Ind. Eng. Chem. Fundam.* **1986**, *25* (2), 269–279.

(9) Knapp, J. P.; Doherty, M. F. Minimum Entrainer Flow for Extractive Distillation: A Bifurcation Theoretic Approach. *AIChE J.* **1994**, *40* (2), 243–268.

(10) Rodríguez-Donis, I.; Gerbaud, V.; Joulia, X. Thermodynamic Insights on the Feasibility of Homogeneous Batch Extractive Distillation. 1. Azeotropic Mixtures with Heavy Entrainer. *Ind. Chem. Eng. Res.* **2009**, *48* (7), 3544–3559.

(11) Rodríguez-Donis, I.; Gerbaud, V.; Joulia, X. Thermodynamic Insights on the Feasibility of Homogeneous Batch Extractive Distillation, 2. Low-Relative-Volatility Binary Mixtures with a Heavy Entrainer. *Ind. Chem. Eng. Res.* **2009**, *48* (7), 3560–3572.

(12) *ProSim Ternary Diagram*; ProSim: Labege Cedex, France, 2005. Available at http://www.prosim.net/en/resources/download.html. (Accessed December 14, 2011).

(13) *Simulis Thermodynamics*; ProSim: Labege Cedex, France, 2007. Available at http://www.prosim.net/en/thermodynamics/simulist.html. (Accessed December 14, 2011).

(14) Gmehling, J.; Onken, U. *Vapor−Liquid Equilibrium Data Collection*DECHEMA Chemistry Data Series; DECHEMA: Frankfürt am Main, Germany, 1977.

(15) *BatchColumn*; ProSim: Labege Cedex, France, 2007. Available at http://www.prosim.net/en/batch/batch.html. (Accessed December 14, 2011).

(16) *CHEMCAD*; Chemstations, Inc.: Houston, TX, 2010. Available at http://www.chemstations.com/. (Accessed December 14, 2011).

(17) Hunek, J.; Gal, S.; Posel, F.; Glavic, P. Separation of an azeotropic mixture by reverse extractive distillation. *AIChE J.* **1989**, *35* (7), 1207–1210.

(18) Lelkes, Z.; Lang, P.; Otterbein, M. Feasibility and sequencing studies for homoazeotropic distillation in a rectifier with continuous entrainer feeding. *Comput. Chem. Eng.* **1998**, *22*, S653–S656.

(19) Varga, V.; Rev, E.; Gerbaud, V.; Lelkes, Z.; Fonyo, Z.; Joulia, X. Batch Extractive Distillation with Light Entrainer. *Chem. Biochem. Eng. Q.* **2006**, *20* (1), 1–24.

(20) Lang, P.; Lelkes, Z.; Otterbein, M.; Benadda, B.; Modla, G. Feasibility studies for batch extractive distillation with a light entrainer. *Comput. Chem. Eng.* **1999**, *23*, S93–S96.

(21) Lelkes, Z.; Lang, P.; Benadda, B.; Moszkowicz, P. Feasibility of Extractive Distillation in a Batch Rectifier. *AIChE J.* **1998**, *44*, 810–822.

(22) Varga, V. Distillation Extractive Discontinue dans une Colonne de Rectification et dans une Colonne Inverse. *Ph.D. Thesis*, L'Institut National Politechnique de Toulouse, Toulouse, France, 2006.

(23) Reshetov, S. A.; Kravchenko, S. V. Statistics of Liquid−Vapor Phase Equilibrium Diagrams for Various Ternary Zeotropic Mixtures. *Theor. Found. Chem. Eng.* **2007**, *41* (4), 451–453.

(24) Frits, E. R.; Lelkes, Z.; Fonyo, Z.; Rev, E.; Markot, M. Cs. Finding Limiting Flows of Batch Extractive Distillation with Interval Arithmetics. *AIChE J.* **2006**, *52* (9), 3100–3108.

(25) Doherty, M. F.; Malone, M. F. *Conceptual Design of Distillation Systems*; McGraw Hill: New York. 2001.

(26) Bernot, C.; Doherty, M. F.; Malone, M. F. Patterns of Composition Change in Multicomponent Batch Distillation. *Chem. Eng. Sci.* **1990**, *45*, 1207–1221.